İSTANBUL TECHNICAL UNIVERSITY ★ GRADUATE SCHOOL OF SCIENCE ENGINEERING AND TECHNOLOGY

COSMO-CLM (CCLM) CLIMATE SIMULATIONS OVER TURKEY: PERFORMANCE EVALUATION AND CLIMATE PROJECTIONS FOR THE 21ST CENTURY

M.Sc. THESIS

Cemre YÜRÜK

Department of Meteorological Engineering

Atmospheric Sciences Programme

Thesis Advisor: Prof. Dr. Yurdanur S. ÜNAL

JANUARY 2017

İSTANBUL TECHNICAL UNIVERSITY ★ GRADUATE SCHOOL OF SCIENCE ENGINEERING AND TECHNOLOGY

COSMO-CLM (CCLM) CLIMATE SIMULATIONS OVER TURKEY: PERFORMANCE EVALUATION AND CLIMATE PROJECTIONS FOR THE 21ST CENTURY

M.Sc. THESIS

Cemre YÜRÜK
(511141005)

Department of Meteorological Engineering

Atmospheric Sciences Programme

Thesis Advisor: Prof. Dr. Yurdanur S. ÜNAL

JANUARY 2017

İSTANBUL TEKNİK ÜNİVERSİTESİ ★ FEN BİLİMLERİ ENSTİTÜSÜ

TÜRKİYE İÇİN COSMO-CLM (CCLM) İKLİM SİMÜLASYONLARI: PERFORMANS DEĞERLENDİRMESİ VE 21. YÜZYIL İKLİM PROJEKSİYONLARI

YÜKSEK LİSANS TEZİ

Cemre YÜRÜK
(511141005)

Meteoroloji Mühendisliği Anabilim Dalı

Atmosfer Bilimleri Programı

Tez Danışmanı: Prof. Dr. Yurdanur S. ÜNAL

OCAK 2017

Cemre Yürük, a M.Sc. student of İTU Graduate School of Science Engineering and Technology student ID 511141005, successfully defended the thesis/dissertation entitled "COSMO-CLM (CCLM) CLIMATE SIMULATIONS OVER TURKEY: PERFORMANCE EVALUATION AND CLIMATE PROJECTIONS FOR THE 21ST CENTURY", which she prepared after fulfilling the requirements specified in the associated legislations, before the jury whose signatures are below.

Thesis Advisor :	**Prof. Dr. Yurdanur S. ÜNAL** İstanbul Technical University	.....
Jury Members :	**Doç. Dr. Barış ÖNOL** İstanbul Technical University	.....
	Yrd. Doç. Dr. Meral DEMİRTAŞ 19 Mayıs University	.....

Date of Submission : 25 November 2016
Date of Defense : 10 January 2017

To my family,

FOREWORD

This is the M.Sc. thesis completed as a requirement of Department of Meteorology Engineering Atmospheric Sciences Program at Istanbul Technical University. In this project, dynamically downscaled climate simulations over Turkey produced with regional climate model COSMO-CLM are presented.

I am very grateful to my supervisor Prof. Dr. Yurdanur S. UNAL for giving me an opportunity to share her knowledge and being tolerant to me during thesis period. I would like to thank Kadir DIRI and Remzi AKYUZ who gave me practical support while installing the model. I am also owing a great thank to CLM-Community and Deutsches Klimarechenzentrum for providing initial and boundary data. I am indebted to Prof. Dr. Sahar SODOUDI, Dr. Bijan FALLAH, Alexander WALTER and Emmanuele RUSSO from Freie University Berlin for answering my all questions. Besides, I would like to extend my thanks to my friends, especially Simge Irem BILGEN and Erkan YILMAZ for their positive energy and motivation. Finally, I thank to my family and Baran Emre SONUC for their encouragement and everlasting support.

November 2016

Cemre YÜRÜK
(Meteorological Engineer)

TABLE OF CONTENTS

Page

ABBREVIATIONS

CCLM : COSMO-CLM
CMIP5 : Coupled Models Intercomparison Project Phase 5
COSMO : Consortium for Small-Scale Modelling
CRU : Climatic Research Unit
ESM : Earth System Model
FAO-DSMW : Digital Soil Map of World
GCMs : General Circulation Models
GLC2000 : Global Land Cover for the year 2000
ICTP : The International Centre for Theoretical Physics
IPCC : Intergovernmental Panel on Climate Change
LM : Local Model
LR : Low Resolution
MPI : Max-Planck-Institut
RCMs : Regional Climate Models
RCP : Representative Concentration Pathways
RegCM : Regional Climate Model
RF : Reference Period
TKE : Turbulent Kinetic Energy
TS : Time Series
TSMS : Turkish State Meteorological Service
WebPEP : Web Interface for Preprocessing External Data Parameters
1D : One Dimensional
3D : Three Dimensional

SYMBOLS

^{o}C	**:** Celcius Degree
CO_2	**:** Corbon Dioxide
μ	**:** Gal-Chen Coordinate
μ_s	**:** SLEVE Coordinate
η	**:** Pressure-based Coordinate
ζ	**:** Terrain-following Coordinate

LIST OF TABLES

Page

LIST OF FIGURES

Page

COSMO-CLM (CCLM) CLIMATE SIMULATIONS OVER TURKEY: PERFORMANCE EVALUATION AND CLIMATE PROJECTIONS FOR THE 21ST CENTURY

SUMMARY

In this study, the results of regional climatology based on NCAR/NCEP Reanalysis and MPI-ESM-LR driven COSMO-CLM (CCLM) simulations over Turkey and its vicinity are presented. The main purposes of this thesis are to ascertain the capability of the non-hydrostatic regional climate model CCLM in capturing temperature and precipitation and also, to investigate the effect of climate change on temperature and precipitation distribution through 21st century by employing the current extreme Intergovernmental Panel on Climate Change (IPCC) scenario, Representative Concentration Pathways 8.5 (RCP8.5).

The simulations are conducted at two different horizontal grid spacings (0.44° and 0.11°). The outputs of earth system model (ESM) MPI-ESM-LR are downscaled to first coarse resolution over mother domain, which covers Turkey and its vicinity. Then, it is downscaled to high resolution over northwestern Turkey for reference period (RF) of 1971-2005 by using CCLM in order to assess the ability of the model to reproduce the climatological features of the region. Moreover, NCAR/NCEP Reanalysis data is also dynamically downscaled by following the same steps to explore the inherent performance of the CCLM for the same region that has complex topography and shorelines. In addition, the future projections are forced by MPI-ESM-LR covering 2011-2100 with proposed changes under IPCC RCP8.5 scenario.

The validation of CCLM is evaluated with respect to various observational data sets. The 0.44° resolution simulations of CCLM for reference period are compared with Climatic Research Unit (CRU) gridded data by interpolating CRU values to CCLM grid. Furthermore, CCLM simulations having 0.11° resolution compared with meteorological observations obtained from TSMS stations after the model results are bilinearly interpolated to stations' location. A focus is put on near-surface conditions and the analyses of the simulations are carried out on annual and seasonal basis.

When the annual and seasonal averages of mean 2-m temperatures are analyzed, it is concluded that both the reanalysis and ESM driven CCLM model results show similar temperature distribution with CRU over the mother domain for 1971-2005. The model evaluation reveals that the coupled CCLM is able to approximately reproduce the observed spatial variation of 2-m temperature over Turkey in winter and autumn seasons that are dominated by cold bias in CCLM_NCEP1. Although the both simulations driven with NCEP1 and ESM have generally larger biases (>2℃) over mountainous regions such as Caucasus Mountains, it underestimates the temperatures (<-2℃) over northeastern part of Turkey. Precipitation analysis with respect to CRU shows that reanalysis driven CCLM produces values close to the spatial variation of the total annual precipitation in the north of Turkey while coupled CCLM simulates consistent values that changes between ± 100 mm in the southern

part of Turkey. Additionally, the dryness of the summer season over Turkey is well captured (± 50 mm) by the both simulations.

CCLM coupled with MPI-ESM-LR gives more consistent results than CCLM forced with NCEP1 in all seasons except summer and also reduces the temperature biases of CCLM_NCEP1 that are colder than TSMS values in winter and autumn seasons by at least 1℃. Besides, comparing the both 0.11° temperature simulations with the TSMS stations on annual and seasonal basis shows that the model has high cold bias in elevated regions. It is observed that the consistency between the model and the observation data increases when the differences are recalculated considering the model topography. On the other hand, reanalysis driven CCLM has generally dry bias whereas coupled model system has wet bias according to TSMS stations. The best performance is observed in spring (0.7 mm) and summer (-16 mm) for CCLM_NCEP1 yet in summer (24 mm) and autumn (15.2 mm) seasons for CCLM_MPI-ESM-LR.

Climate in Turkey is expected to be noticeably affected by 21st century global warming and the warming in the second half of the century is predicted to accelerate more steeply. Through the end of century, significant warming (>6℃) particularly over eastern (for 0.44° resloution) and inland (for 0.11° resloution) parts of Turkey is expected in summer season. However, this climate change does not only refer to increasing temperatures but also to changing precipitation regimes. There is a tendency towards a larger relative decrease of summer precipitation at higher elevations, but there are exceptions to this as well. Drier conditions exceeding 90 mm are apparent over the mountainous regions in 2071-2100 period compared to previous periods, especially for the projections of 0.11° resolution.

TÜRKİYE İÇİN COSMO-CLM (CCLM) İKLİM SİMÜLASYONLARI: PERFORMANS DEĞERLENDİRMESİ VE 21. YÜZYIL İKLİM PROJEKSİYONLARI

ÖZET

İklim modelleri, iklim sistemi bileşenleri arasındaki karmaşık etkileşimleri anlamaya yarayan birincil araçlardır. Öte yandan, emisyon senaryolarının yardımıyla iklim sistemi bileşenlerinin gelecekteki durumunu simüle etmek için kullanılmaktadır. İklim değişikliği küresel bir olgu olmasına rağmen, iklim değişikliğinin etkileri yerel ve bölgesel ölçekte de hissedilebilmektedir. Çözünürlüğü 100 km ile 400 km arasında değişen genel dolaşım modellerinin (GCM) yardımı ile bölgesel ölçekte iklim değişimlerini çözebilmek ve bu bölgesel etkileri değerlendirmek zordur. Bu nedenle, bölgesel iklim modelleri (RCM) ülke çapında gelecek projeksiyonlarını gerçekleştirmek ve politik çözümler üretmek için gereklidir. Yaygın bir yöntem olan dinamik ölçek küçültme yöntemi ile, bölgesel iklim modelleri genel dolaşım modellerinin ölçeğini dinamik olarak küçültmektedir. Böylece bölgesel iklim modelleri, kıyı şeritleri gibi yüzey heterojenliklerinden etkilenen alanlar hakkında daha ayrıntılı bilgiler sağlamakta ve orta ölçekli atmosferik olayları genel dolaşım modellerinden daha iyi yakalamaktadır.

Çalışmanın genel amacı Türkiye ve batısı için günümüz ve gelecek koşulları iklim simülasyonlarını gerçekleştirmektir. Bu amaç için hidrostatik olmayan sınırlı alan modeli COSMO-CLM (CCLM) iklim modeli koşturulmuştur. Açılımı Consortium for Small-scale Modeling olan COSMO modeli, CLM Topluluğu (CLM-Community) tarafından Alman Meteoroloji Servisi'nin Bölgesel Modeli (Local Model) kullanılarak geliştirilmiştir. COSMO modeli, herhangi bir ölçek yaklaşımı kullanılmadan nemli atmosferdeki sıkıştırılabilir akışı tanımlayan ilkel termo-hidrodinamik denklemlere dayanmaktadır. Model denklemleri dönen coğrafi koordinatlarda formüle edilmiş ve yüzeyi takip eden yükseklik koordinatlarında genelleştirilmiştir. Atmosferdeki bazı fiziksel süreçler parametreleştirme şeması ile hesaba katılmıştır.

Çalışma kapsamı yerel iklim koşullarının ortaya koyulması olduğundan 0.11° (yaklaşık 12 km) çözünürlüğe kadar inilmiştir. Simülasyonlar 1971'den 2005 yılının sonuna kadar olan 35 yıllık bir zaman aralığını kapsamaktadır. Ancak yüksek çözünürlükte modelin başlangıç birkaç yılı spin up zamanı olarak alınmakta olup analizlerde kullanılmamaktadır. Model için kullanılan koordinatlar dıştaki çalışma alanı için Türkiye esas alınarak, içteki çalışma alanı için ise Türkiye'nin batısı baz alınarak seçilmiştir.

Hem günümüz hem de gelecek küresel iklim simülasyonları, CCLM sınırlı alan modelinin Max-Plank Meteoroloji Enstitüsü (Max-Planck-Institut for Meteorology) tarafından geliştirilen ve CMIP5 (Coupled Models Intercomparison Project Phase 5) arşivinde yer alan MPI-ESM-LR yer sistem modeli çıktılarıyla zorlanmasından elde edilmiştir. MPI-ESM yer sistem modeli, atmosferi temsil eden ECHAM6 ve buz-okyanus ilişkisini içeren MPIOM genel sirkülasyon modellerinden oluşmaktadır.

Bunların yanı sıra MPI-ESM-LR, yer yüzeyi ve bitki örtüsünün atmosfer ile etkileşimini kapsayan JSBACH; okyanus biyogeokimyasını temsil eden HAMOCC alt sistem modellerini içermektedir. Düşük çözünürlükteki bu konfigürasyon, atmosfer için T63/1.9° yatay çözünürlükte olmasından dolayı 0.11° çözünürlüğe ulaşabilmek adına 2 aşamalı dinamik yuvalama stratejisi izlenmiştir. Öncelikle CCLM, MPI-ESM-LR ile zorlanarak 0.44° (yaklaşık 50 km) çözünürlükte simülasyonlar elde edilmiştir. Daha sonra 3 saatlik aralıklar ile yazdırılan 0.44° simülasyonları ile zorlanan CCLM modeli 0.11° çözünürlükte koşturulmuştur. Bunun yanı sıra, karmaşık topografya ve kıyı şeritlerine sahip aynı bölge ve aynı referans dönemi için CCLM modelinin performansını keşfetmek amacıyla bir kez de NCAR/NCEP Reanalysis veri seti ile dinamik ölçek küçültme yöntemi uygulanmıştır.

0.44° çözünürlüğe sahip simülasyonlar, küresel veri setlerinden biri olan ve 0.5° grid çözünürlüğüne sahip İklim Araştırma Birimi (CRU) veri setinin ortalama sıcaklık ve yağış verileri ile karşılaştırılarak Türkiye gibi kompleks bir topoğrafya üzerinde modelin tutarlılığı irdelenmiştir. Bunun yanı sıra, 0.11° çözünürlüğe sahip simülasyonlar için Türkiye'ye ait ortalama sıcaklık gözlemi yapan 372 Meteoroloji Genel Müdürlüğü (MGM) istasyonundan, %20'den fazla eksik veri bulunduran istasyonlar elenerek, geriye kalan 217 noktadaki gözlem verisinden çalışma alanında kalan 48 istasyona ait veriler, istasyonlara en yakın gridlerdeki model çıktıları ile karşılaştırılarak yanlılık analizi yapılmıştır. Aynı yöntem ile yağış için Türkiye genelinde bulunan 283 istasyondan en çok veriye sahip 212 istasyon hesaplanmış ve bu 212 istasyon içerisinden 48 istasyonun ise çalışma alanı içerisinde kaldığı tespit edilmesinin ardından yağış için de yanlılık analizi yapılmıştır. Ayrıca ortalama sıcaklık için model yüksekliklerinden istasyon yükseklikleri çıkarılmış, bu değerler sıcaklığın yükseklik ile değişimini ifade eden ortalama lapse rate (6.5℃/km) ile çarpıldıktan sonra model çıktılarına eklenmiştir. Bu düzeltmenin sonucunda elde edilen yeni model sonuçlarının, istasyon değerleri ile tekrar farkı alınarak model topoğrafyasının sıcaklık ile ilişkilendirilmesi sağlanmış ve Türkiye'nin batı bölgesinde model taraflılığı test edilmiştir.

2-m sıcaklıkların yıllık ve mevsimsel ortalamalarına bakıldığında hem reanaliz veri seti ile koşturulan hem de MPI-ESM-LR yer sistem modeli ile kuple edilen CCLM model sonuçlarının CRU gözlem verisetine göre, 0.44° çözünürlüğe sahip ana çalışma alanı üzerinde benzer sıcaklık dağılımı ortaya koymaktadır. Yıllık sıcaklık ortalamaları, kuple edilen model simülasyonlarının Türkiye üzerinde daha tutarlı (± 1℃) olduğunu göstermektedir. Benzer şekilde reanalizle zorlanan model sonuçlarında kış ve sonbahar mevsimlerinde soğuk yanlılığın hâkim olduğu Türkiye'de kuple edilen model, değerleri daha tutarlı hale getirmektedir. Bu karşılaştırmalarda en çok dikkat çeken, her iki şekilde de koşturulan CCLM modelinin genellikle Kafkas Dağları gibi dağlık bölgelerde daha büyük yanlılığa (>2℃) sahip olmasına rağmen yükseltinin fazla olduğu Türkiye'nin kuzeydoğusundaki sıcaklıkları daha düşük (<-2℃) üretmesidir. Modelin CRU'ya göre yağış performans analizi, reanaliz verisiyle zorlanan CCLM'in Türkiye'nin kuzeyinde; kuple edilen CCLM'in ise Türkiye'nin güneyinde yıllık toplam yağışın mekansal değişimine yakın değerler (± 100 mm) simüle ettiğini göstermektedir. Her iki simülasyonda da Kafkas Dağları üzerinde 800mm'yi aşan pozitif yanlılık göze çarpmaktadır. Mevsimsel toplamlar ele alındığında ise Türkiye üzerinde genellikle CRU'ya yakın değerler üreten CCLM simülasyonları, en tutarlı yağış değerlerini yaz mevsimde ortaya koymaktadır.

0.11° çözünürlüğe sahip sıcaklık simülasyonları yıllık ve mevsimlik bazda TSMS istasyonlarıyla karşılaştırıldığında modelin yüksek bölgelerde soğuk taraflılığı fazla çıkmış; model topoğrafyasını göz önünde bulundurarak farklar tekrar hesaplandığında ise model ile gözlem verileri arası tutarlılığın arttığı gözlenmiştir. Yükselti düzeltmesi yapıldıktan sonra 48 istasyon üzerinde hesaplanan yıllık sıcaklık ortalamaları CCLM_NCEP1 için -1.3℃'den -0.5℃'e; CCLM_MPI-ESM-LR için -0.49℃'den 0.3℃'e düşürülmüştür. Bunun yanı sıra, yer sistem modeli ile kuple edilmiş CCLM yaz mevsimi dışındaki bütün mevsimlerde NCEP1 ile koşturulan CCLM'den daha tutarlı sonuçlar vermekte, CCLM_NCEP1'in özellikle kış ve sonbahar mevsimlerinde TSMS değerlerine göre daha soğuk tahmin ettiği istasyonlardaki sıcaklık yanlılığını en az 1℃ azaltmaktadır. Yağış değerlerini ise gözlemlere kıyasla genellikle daha yüksek tahmin etmektedir. Buna karşılık reanaliz verisi ile zorlanan bölgesel iklim modeli hem yıllık hem de mevsimlik toplam yağışları çoğu istasyon noktasında daha düşük üretmektedir. Her iki simülasyon da, ± 25 mm'lik yanlılık değeri ile yaz mevsiminde en iyi performansını göstermektedir.

Çalışmanın diğer bir amacı, sıcaklık ve yağış parametrelerindeki değişimleri değişen iklim koşulları altında ortaya koymaktır. Bu nedenle projede, gelecek iklim beklentileri için Hükümetlerarası İklim Değişikliği Paneli'nin (Intergovernmental Panel on Climate Change - IPCC) Temsili Konsantrasyon Rotaları (Representative Concentration Pathways) olarak adlandırılan yeni gelecek emisyon senaryoları RCP2.6, RCP4.5, RCP6 ve RCP8.5 arasından RCP8.5 senaryosu seçilmiştir. RCP8.5 rotası, sera gazı emisyonlarındaki artış sonucunda 2100 yılına kadar CO_2 konsantrasyonunun 940 ppm'e erişeceğini göz önüne aldığından sıcaklıklar açısından en kötümser senaryo olarak adlandırılır. Böylelikle, en kötü koşullar altında lokal iklimdeki, özellikle sıcaklık ve yağışlardaki değişimler ortaya koyulmaya çalışılmaktadır.

Türkiye'de iklimin 21. yüzyılın küresel ısınmasından belirgin şekilde etkileneceği ve yüzyılın ikinci yarısındaki ısınmanın daha hızlı bir şekilde gerçekleşeceği tahmin edilmektedir. Özellikle yaz aylarında yüzyılın sonuna doğru Türkiye'nin doğusunda (0.44° çözünürlüğe sahip simülasyonlara göre) ve iç bölgelerinde (0.11° çözünürlüğe sahip simülasyonlara göre) 6℃'yi aşan ciddi bir sıcaklık artışı beklenmektedir. Bununla birlikte, bu iklim değişikliği sadece artan sıcaklıkları değil, aynı zamanda değişen yağış rejimlerini de ifade etmektedir. 1971-2005 referans periyoduna göre yüksek topoğrafyaya sahip bölgelerin yaz yağışlarında büyük bir miktarda azalma eğilimi vardır. Bilhassa 0.11° çözünürlüklü iklim projeksiyonlarına göre, 2071-2100 periyodunda diğer dönemlere kıyasla dağlık bölgelerin daha kurak koşulların (90 mm'yi aşan) etkisi altında kalacağı aşikârdır.

1. INTRODUCTION

The climate models are utilized as primary tools in order to comprehend the complex interaction among the climate system components. On the other hand, they are used to mimic the future state of the climate system components with the help of emission scenarios. Thus, they serve as main tools for studying climate change.

Although climate change is a global phenomenon, the impacts of climate change can be also felt at the local and regional scale. It is hard to resolve climate variations in regional scale and assess these regional impacts with the help of general circulation models (GCMs) due to primarily their coarse spatial resolution ranging between 100 km and 400 km. Therefore, regional climate models (RCMs) are essential for making future projections and policy decisions in country scale. As a common procedure, GCMs outputs are transferred to limited areas with RCMs by dynamical downscaling method (Von Storch et al, 2000; Murphy, 1999) to obtain fine scale information. Thus, regional climate models provide much more detailed information influenced by surface heterogeneities such as coast lines, and they better capture mesoscale atmospheric processes than the general circulation models allow.

Recently, climate change studies have been accelerating with the developing RCMs technology. They do not only consist of future projections but also include present-day simulations. Present-day simulations are necessary to evaluate model performance and sensitivity, to estimate confidence intervals for certain model parameters and sub-regions and to analyze future projections according to reference simulations. Therefore, the numerous studies in the literature focus on analyzing the regional climate model performance by applying different sensitivity tests (For instance, Bucchignani et al. (2016), Roesch et al. (2008), Jaeger et. al. (2008), Geyer (2014), etc.)

Sensitivity analysis of ERA-Interim driven COSMO-CLM over Middle East-North Africa (CORDEX-MENA) domain with 0.44-degree resolution was evaluated between 1980 and 1984 in terms of temperature (compared with CRU, UDEL,

MERRA), precipitation (compared with CRU, GPCC, GPCP, UDEL, MERRA), cloud cover (compared with CRU, MERRA) and mean sea level pressure (compared with MERRA) by comparing 26 set of CCLM runs with the combination of ground observations, satellite products and reanalysis data. It is found that the model performance is improved by configurations (w and z) with alternative albedo, which is function of dry and saturated soil, and aerosol optical depth (AOD) (NASA GISS AOD distributions) options. Running COSMO-CLM with a higher albedo value of the laminar boundary layer (LBH) parameter (r and s) gave a significant contribution to the improvement of cloud cover with respect to the reference configuration (a) (Bucchignani et al, 2016).

Meissner et al. (2009) evaluated the sensitivity of the regional climate model COSMO-CLM, which was driven by the ERA40 and NCEP reanalysis data sets respectively and with both 7 km and 14 km horizontal resolutions, over southwestern Germany between the period 1991 and 2000. They claimed that the simulation results driven with the NCEP reanalysis data produced larger discrepancies between temperature and precipitation values and observations compared to the ones forced with the ERA40 reanalysis data. The effect of driving data on simulation results is more significant than the effect of increasing resolution.

Geyer (2014) presents the atmospheric part of coastDat2, which was performed by COSMO-CLM between 1948 and 2012. The model is forced with NCEP1 initial and boundary data. 2-m temperature, total precipitation, wind speed and cloud cover simulations that have 0.22-degree resolution are compared with E-OBS, CRU, GPCC and REGNIE data sets. Lindenberg, Germany station data is used for evaluation of boundary layer height. It is shown that the model underestimates diurnal temperature range for most of the regions, excluding North Africa. In summer, the model has more negative bias (precipitation) over southeastern Europe in comparison with GPCC than E-OBS.

The study on climatological analysis and interannual variations of 2-m temperature and precipitation is done for Europe by using CCLM with different set ups. It argues that CCLM conspicuously underpredicts 2-m temperature in spring and summer over most of Europe above approximately 40°N while overpredicts 2-m temperature in Northern part of Europe during winter. Europe is dominated by a pronounced wet bias for all seasons, excluding dry summer bias from Italy to the Black Sea. It is

revealed that temperature and precipitation biases for both mean and interannual variability critically depend on ensemble members selected for the evaluation. Therefore, it is suggested that one model is inadequate to assess the performance of the model in simulating climate extremes (Roesch et al, 2008).

Jaeger et al. (2008) also analyzed ERA40-driven CLM simulations performed with different model versions for Europe. In summer season, CLM version 2.4.6 produces generally warm and dry bias. On the contrary, CLM version 4.0 simulates abnormal cold and wet bias. They suggest that this can arise from a strong underestimation of the net radiation that is connected to the overestimation of cloud cover. Furthermore, CLM 2.4.6 simulations performed with different spatial resolutions that are 0.44° and 0.22°. It is concluded that the shifting to higher resolution does not give clear benefit for the analyzed fields. It only helps to resolve fine-scale structures better.

Another study, which focuses on near-surface parameters, reveals that over all 8 subdomains, COSMO-CLM model forced with both ERA40 and HadCM3 overestimates mean lapse rates compared to E-OBS data between 1961-2000, particularly in Alps (AL), France (FR) and Eastern Europe (EA) sub-regions. Most of regions below 100 m elevation are exposed to increase in precipitation while high elevations are exposed to dry biases with respect to S2001 high-resolution dataset. In addition to evaluation results, it is asserted that the near-surface warming throughout 21st century intensifies with the elevation whereas precipitation change becomes evident mostly with season, intermittently with elevation. Winter precipitation tends to largely increase with the elevation, except in AL, FR and Scandinavia (SC) sub-regions while summer precipitation relatively decreases at low elevations. (Kotlarski et al, 2012). As a precursor study done by two regional climate models for climate change in the European Alps, Giorgi et al. (1997) claimed that larger warming signal strongly hinges upon higher elevations. In addition to this, a review study on Alpine region, which is exposed to a strong topographic variability, has been provided by Gobiet et al. (2014). 22 RCM projections with 25 km horizontal resolution are taken from the EU FP6 Integrated Project ENSEMBLES that concerns future greenhouse gas with A1B emission scenario. It is shown that winter precipitation increases while summer precipitation decreases more in the second half of the 21st century than in the first half. Moreover, 0.25℃ warming is expected per decade until the mid of the 21st century and accelerates to 0.36℃ per decade afterwards.

Most of the recent studies use new scenario approach to take into account future concentrations of greenhouse forcings. Representative Concentration Pathways (RCPs) are defined for the Fifth Assessment Report of the IPCC (Moss, et al., 2010). They assume target radiative forcing by the end of the 21st century whereas SRES scenarios lead to socio-economic effects. For instance, RCP8.5 suppose a rising radiative forcing of 8.5 W/m^2 in 2100 relative to pre-industrial conditions (Jacob et al, 2014).

ERA-Interim is dynamically downscaled respectively to 0.22, 0.125 and 0.0715 degree resolutions with COSMO-CLM model over Italy. 2-m temperature has generally good agreement with observations within the period 1980-2011. However, according to E-OBS the model underestimates winter temperatures whereas overestimates summer temperatures. Moreover, it is indicated that biases are reduced due to the increase in resolution. In addition to ERA-Interim driven simulations, two simulations having 0.0715° resolution are forced by GCM CMCC-CM over the period 1971-2100 in accordance with RCP4.5 and RCP8.5 scenarios. Scenarios, especially RCP8.5, exhibit significant warming and decreasing precipitation in Italy at the end of 21st century (Bucchignani et al, 2016).

Many modeling studies have been carried out to investigate climate variability in Turkey. For instance, Bozkurt et al. (2012) evaluated the high-resolution climatology of the dynamically downscaled outputs from the three different GCMs that are MPI-ECHAM5, NCAR-CCSM3 and HadCM3 for the 1961-1990 reference period by using RegCM3. The simulations have 27 km horizontal resolution with 144×100 grid points. Additionaly, Onol et al. (2014) analyzed human-induced climate change over the Eastern Mediterranean–Black Sea region for the 21st century by dynamically downscaling the same three GCMs under A2, A1FI and B1 scenarios. Unal et al. (2001); Karaca et al. (2003); Onol and Semazzi (2009); Unal et al. (2006-2010); Bozkurt and Sen (2011); Onol (2012); Onol and Unal (2014) and MGM (2015) are other examples of climate modelling studies that includes Turkey. However, all of the studies are performed by Regional Climate Model (RegCM) maintaned under the International Centre for Theoretical Physics (ICTP). In this work, a non-hydrostatic regional climate model CCLM, which was developed by CLM-Community, has been used as a precursor to lead many studies in the future which will be done by CCLM for Turkey. Turkey is located in the Mediterranean Basin that belongs to semi-arid

regions. This type of regions has been identified as most climatically sensitive areas and Giorgi characterized Mediterranean region one of the 'hot spots' of the future climate change (2006). Besides, Mediterranean Basin comprises of a landmass surrounded by Mediterranean and the Black Sea. These saline water bodies gradually exchange with the rest of the oceans which makes it a semi-enclosed system (Hatzianastassiou et al, 2016).

The goals of this study are firstly to test the performance of the CCLM for the reference period and secondly to give insight about climate change by applying emission scenario to future simulations for the 21st century. The study focuses on typically near surface meteorological variables, such as air temperature and precipitation used within the most of the climate studies. The reason is that they are common variables to validate numerical models since they have been measured for ages and have direct influence on human beings (Roesch et al, 2008). This thesis is structured in following way. The description of the regional climate model CCLM, the configuration options and the model domain and also the data, which are used in order to validate the model and used as lateral forcing, are introduced in section 2. The evaluation of the model, future projections, analyses and their results are presented in section 3. Finally, the outcomes of the study are summarized in conclusion section 4.

2. DATA AND METHOD

2.1 Regional Climate Model COSMO-CLM (CCLM)

The Consortium for Small-scale Modeling (COSMO) was developed from the Local Model (LM) of the German Meteorological Service by CLM-Community as a non-hydrostatic limited-area atmospheric model. The general aim is to be used for both operational numerical weather prediction (NWP) and research applications on the meso-β and meso-γ scale especially by the members of the consortium. However, it is used by other national (hydro-) meteorological services, universities and research institutes within a license agreement.

The COSMO model is based on primitive thermo-hydrodynamical equations that define compressible flow in a moist atmosphere without using any scale approximations. The basic equations are written in advection form and the continuity equation is replaced by a prognostic equation for the perturbation pressure. The COSMO model is designed for meso-β and meso-γ scales, where non-hydrostatic effects begin to play an important role in the development of atmospheric flow. The model equations are formulated in rotated geographical coordinates and in a terrain-following coordinate system using a generalized vertical coordinate ζ. Three options are offered for the terrain-following coordinate, which are the base-state pressure-based height coordinate (η), height-based hybrid Gal-Chen coordinate (μ) for small-scale non-hydrostatic modelling (Gal-Chen and Sommerville, 1975) and exponential height-based hybrid SLEVE (Smooth Level VErtical) coordinate μ_s according to the Schär et al. (2002). The model variables are staggered on an Arakawa-C/Lorenz grid with scalars defined at the centre of a grid box and the normal velocity components defined on the corresponding box faces (Doms and Baldauf, 2015). (i.e. the deviation of pressure from the reference state). The model equations are solved numerically using the traditional second-order finite differences. For the time integration, the model uses 2nd order leapfrog horizontally explicit (HE) – vertically implicit (VI) time-split integration scheme (Skamarock and Klemp, 1992) as a default. There is another option for a three time-level 3D semi-implicit scheme (Thomas et al, 2000).

Additional options are also availiable for a dynamical core in order to solve compressible Euler-equations. The first one is 2nd and 3rd order two time-level Runge-Kutta split-explicit scheme that is based on time-splitting approach of Wicker and Skamarock (2002) whereas the second one is a Total Variation Diminishing (TVD) variant of a 3rd order Runge-Kutta split-explicit scheme (Liu et al, 1994). The various physical processes in the atmosphere are taken into account with parameterization schemes such as grid-scale clouds and precipitation, subgrid-scale cloudiness, radiation, moist convection, shallow convection, subgrid-scale turbulence and surface fluxes.

The CLM-Community improved the COSMO-Model to be capable of long-term simulations so it is called COSMO model in CLimate Mode (COSMO-CLM or CCLM). The COSMO model sources are same with the source codes of each CCLM components. The model has been utilized for spatial resolutions ranging between 1 and 50 km and time scales up to centuries. One-way nesting for the lateral boundary is formulated by the Davies (1976) relaxation technique. This technique is based on the nudging the specified solutions in a defined boundary zone to the interior solutions of the model, and the nudging is accomplished by a relaxation term added to the equations (COSMO, 2011). CCLM Input (INT2LM), which is an interpolation program, computes the input data for CCLM for preprocessing. INT2LM interpolates and adjusts the coarse grid data to the orography on the CCLM grid. In order to calculate required CCLM input, INT2LM utilizes two data sources. One of them is climatological constant data from the external data set and the other one is initial and boundary data from a coarse resolution model. The simulation domain has to be defined and the external data for that model grid must be obtained to initiate the simulation run. Therefore, there is an available interactive tool WebPEP (Web interface for preprocessing external data parameters) that creates the external parameter file by using the program EXTPAR. Initial and boundary data, which covers a larger area than the simulation area of a chosen CCLM domain, is necessary for the CCLM. GCM, RCM, CCLM (in case of double nesting) and reanalysis data can be used as an initial and boundary data. Table 2.1 shows the required meteorological variables as an input data for the INT2LM.

Table 2.1 : List of essential variables needed for INT2LM.

Variable	Long Name
FIS	Surface geopotential height
FR_LAND	Land-sea fraction
PS	Surface pressure
QV	Specific humidity
T	Temperature
U	U-component of wind
V	V-component of wind

2.2 The Model Domains and Configurations

The computational model domain and topography are shown in Figure 2.1. Horizontal resolutions of 0.44° and 0.11° are used respectively for the dynamical nesting. Two simulations for the reference period were performed over the time period 1971-2005. For the first simulation, initial and boundary conditions were provided by NCEP/NCAR Reanalysis I, which has three-dimensional (3D) variational analysis on a spectral grid with triangular truncation of 62 waves and a spatial resolution of 2.5°×2.5° with 28 levels (Dee et al, 2016). For the second simulation, initial and boundary conditions were provided by MPI-ESM-LR earth system model developed by Max-Planck-Institut for Meteorology. MPI-ESM-LR has the lowest resolution among three different configurations prepared for CMIP5. MPI-ESM earth system model comprises of ECHAM6 atmospheric model component with T63/1.9° horizontal resolution and MPIOM global ocean component using bipolar grid with 1.5° resolution (Giorgetta et al, 2013). In addition to these components, JSBACH represents interaction between land, vegetation and atmosphere whereas HAMOCC performs marine biogeochemistry. The future simulation covering the time period 2011-2100 was also forced by the MPI-ESM-LR in accordance with the Intergovernmental Panel on Climate Change (IPCC) Representative Concentration Pathways 8.5 (RCP8.5) scenario.

The first two years of each nested simulations were selected as “spin-up” period after checking the soil moisture content produced by the CCLM. The soil moisture reached an equilibrium in two years and thus, these two years were discarded in the validation phase.

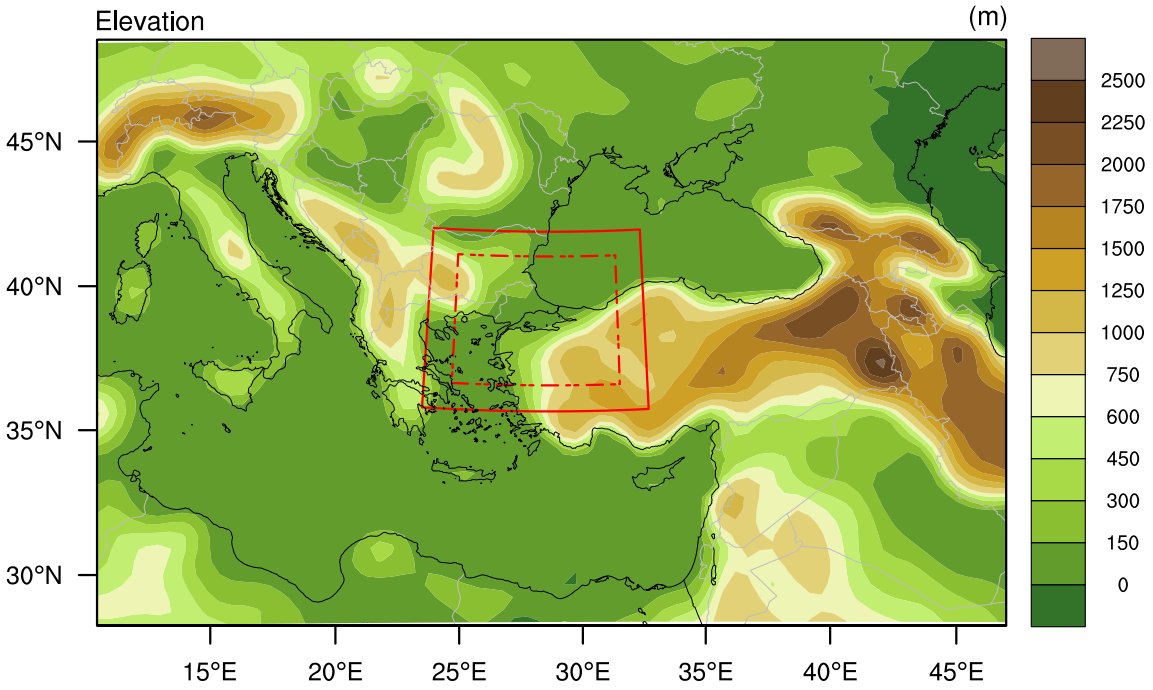

Figure 2.1 : Simulation domains CCLM and elevation (given in meters) with respect to 0.44° resolution. The dashed red frame shows the 10 grid wide sponge zone.

The model configurations for CCLM prepared on the basis of previous studies for Europe and adopted for all the simulations performed in this study (Table 2.2). The computational model domain was determined before running the model and external data set was prepared depending on the resolution of simulations. The external data was created separately for 0.44° and 0.11° resolutions by using interactive web interface WebPEP. Global Land Cover Map for the year 2000 (GLC2000), which has 1 km, resolution was utilized while creating external data. GLC2000 was produced by Joint Research Centre collaborating with a network of international research partners using data acquired by the SPOT4 Vegetation sensor (Bartholome, et al., 2002). In addition to land use data, soil characteristic data set was taken from Digital Soil Map of the World (FAO-DSMW) based on FAO-UNESCO Soil Map of the World (FAO-Unesco, 1974). It was intersected with a template containing water related features (coastlines, lakes and glaciers etc.) at 1:5.000.000 scale and with a Country Boundaries map from the World Data Bank II at 1:3.000.000 scale. Only dry and saturated soil albedo, MODIS dry&sat was given to the model as input of solar surface albedo. For the aerosol climatology, NASA/GISS data set was used. As a result of Global Aerosol Climatology Project (GACP), 23-year global aerosol climatology was assembled from channel-1 and channel-2 AVHRR data and complemented by data from other satellites, field observations and chemical-

transport modeling for the purpose of global and regional modeling studies and interpretation of the global distribution of aerosols, their properties and variations (GACP, 2016)

3rd order, two time-level Runge-Kutta scheme and height based hybrid Gal-Chen coordinate system were used. This Runge-Kutta scheme is also used for the COSMO-DE and COSMO-EU (Schättler et al, 2016). The number of vertical levels in the atmosphere was set to 40 while the number of soil levels was adjusted to 9. The default Tanre aerosol, which provides constant distribution for rural, urban, desert areas and the sea, and the default albedo treatment that is function of soil type were chosen.

Table 2.2 : Selected options for the configuration of CCLM.

Content	Domain	
Horizontal Resolution	0.44°	0.11°
Grid Cell	ie=77, je=50	ie=70, je=60
Vertical Levels	40μ level	40μ level
Corner Coordinates	27.24 N, 10.18 E	37.35 N, 23.35 E
Time Interval	240 sec	120 sec
SST Type	NCEP1/MPI-ESM-LR	FNEST
Data Set Type	NCEP1/MPI-ESM-LR	FNEST
Microphysics Scheme	Two-category Ice Scheme	Two-category Ice Scheme
Convection Scheme	(Tiedtke, 1989)	(Tiedtke, 1989)
Radiation Scheme	(Ritter and Geleyn, 1992)	(Ritter and Geleyn, 1992)
Vertical Turbulent Diffusion Scheme	1D TKE: (Sommeria and Deardorff, 1977)	1D TKE: (Sommeria and Deardorff, 1977)
Surface Transfer Scheme	Diagnostic TKE	Diagnostic TKE
Land Surface Scheme	TERRA-ML	TERRA-ML
Land Use	GLC2000: (Joint Research Centre, 2003)	GLC2000: (Joint Research Centre, 2003)
Periods	RF: 19710101 – 20051231 RCP8.5: 20110101 – 21001231	

Throughout this study, the individual simulations will be identified by the model plus the driving model. For instance, the CCLM simulation forced with NCAR/NCEP Reanalysis I will be referred as *CCLM_NCEP1*.

2.3 Data

2.3.1 Global Climate Datasets

In this study, version 3.23 of Climatic Researh Unit (CRU) time series (TS) dataset was used in order to compare model simulations over larger domain. The dataset was produced by CRU at University of East Anglia and released in 2015. This version is updated version of 2014 dataset. In addition to that, some new stations inserted just for temperature and precipitation. The CRU TS 3.23 data, which cover the period of 1901-2014, consist of monthly observational values gridded on high-resolution (0.5x0.5 degree) grids. These montly fields are calculated from daily or sub-daily data by National Meteorological Services and other external agents for all land areas, excluding Antarctica. All CRU TS output files includes actual valus, not anomalies (University of East Anglia Climatic Research Unit, 2015). The six mostly independent climate variables in the dataset. They are mean temperature (tmp), diurnal temperature range (dtr), precipitation (pre), vapour pressure (vap), cloud cover (cld) and rainday (wet) frequency. Maximum (tmx) and minimum (tmn) temperatures are arithmetically derived from temperature and daily temperature range while potential evapotranspiration (pet) is estimated from a variant of the Penman–Monteith method. Moreover, frostday (frs) counts are calculated from minimum temperature (Harris et al, 2014).

2.3.2 Meteorological Observations

Turkish State Meteorological Service (TSMS) mainly takes the responsibity for the coordination and maintenance of the meteorological observation network in Turkey. TSMS started to found its first network around 1920s. In the beginning, it had a very basic network but then the network has spread gradually country-wide. Nevertheless, the notable expansion of the network has begun after 1960s. The conventional meteorological stations have been replaced progressively with the automatic weather stations after 2007.

In this study, temperature data were provided from 217 stations out of overall 372 TSMS stations in Turkey. These stations were selected according to the criteria that each station should have 80% non-missing values within the interested period. However, only 48 of them falls into the computational domain with 0.11° resolution. For the precipitation data, the same method was applied and 212 stations were

satisfying the proposed missing value constraint out of 283 TSMS stations but only 48 stations remain between the domain boundaries. Table 2.3 lists the number, name, latitude, longitude and height of each meteorological station which belongs to TSMS. Temperature and precipitation share same stations so same stations are taken into account in calculations.

Table 2.3 : Station number, name, latitude, longitude and elevation (given in meters) of the each TSMS station in northwestern Turkey.

Station Number	Station Name	Latitude	Longitude	Elevation
17015	Akcakoca	41.08	31.17	10
17022	Zonguldak	41.45	31.78	135
17050	Edirne	41.68	26.55	51
17052	Kirklareli	41.74	27.22	232
17054	Corlu	41.16	27.82	183
17056	Tekirdag	40.96	27.50	4
17059	Kumkoy	41.25	29.04	38
17061	Kirecburnu	41.15	29.05	59
17062	Goztepe/Ist	40.97	29.06	16
17066	Kocaeli	40.77	29.93	76
17069	Sakarya	40.77	30.39	30
17070	Bolu	40.73	31.60	743
17072	Duzce	40.84	31.15	146
17110	Gokceada	40.19	25.91	79
17111	Bozcaada	39.83	26.07	30
17112	Canakkale	40.14	26.40	6
17114	Bandirma	40.33	28.00	63
17116	Bursa	40.23	29.01	100
17119	Yalova	40.66	29.28	4
17120	Bilecik	40.14	29.98	539
17145	Edremit	39.59	27.02	21
17155	Kutahya	39.42	29.99	969
17175	Ayvalik	39.31	26.69	4
17180	Dikili	39.07	26.89	3
17184	Akhisar	38.91	27.82	92
17186	Manisa	38.62	27.40	71
17188	Usak	38.67	29.40	919
17190	Afyonkara	38.74	30.56	1034
17608	Uzunkopru	41.26	26.69	52
17610	Sile	41.17	29.60	83
17619	Bahcekoy	41.16	28.98	130
17631	Luleburgaz	41.35	27.31	46
17632	Ipsala	40.92	26.38	10
17636	Florya	40.98	28.79	37
17638	Kartal	40.91	29.16	18
17662	Geyve	40.52	30.30	100
17674	Gonen	40.11	27.64	37
17679	Nallihan	40.17	31.33	650
17695	Keles	39.92	29.23	1063
17700	Dursunbey	39.58	28.63	637
17702	Bozuyuk	39.90	30.05	754
17704	Tavsanli	39.54	29.49	833
17726	Sivrihisar	39.45	31.54	1070
17742	Bergama	39.11	27.17	53
17748	Simav	39.09	28.98	809
17752	Emirdag	39.01	31.15	983
17792	Salihli	38.48	28.12	111
17796	Bolvadin	38.73	31.05	1018

3. ANALYSIS AND RESULTS

3.1 Performance Evaluation of The Model

3.1.1 Evaluation of 0.44° simulations

In this section, comparison of NCEP/NCAR Reanalysis 1 driven CCLM model simulations with CRU gridded data is presented for the purpose of demonstrating whether the model outputs represent truly the mean temperature and precipitation over the Turkey or not. In order to compare the model with CRU observations, CRU data was interpolated to CCLM model grids by using bilinear interpolation technique. The annual averages, standard deviations and seasonal averages of temperature and precipitation were analyzed for the period of 1971-2005. The rows named by "DJF", "MAM", "JJA" and "SON" in the figures represent the seasons winter, spring, summer and fall, respectively.

3.1.1.1 Temperature

When the annual temperature distributions are analyzed, the lowest temperatures are seen over Caucasus Mountains and northeastern part of Turkey whereas the highest temperatures are observed over Iraq (Figure 3.1). However, the model (CCLM_NCEP1) predicts warmer temperatures than CRU over these regions. The positive bias reaches up to 4℃ over Caucasus Mountains. Moreover, both the model and CRU temperatures show increasing tendency from the east to the west of Turkey between the periods of 1971-2005. The CCLM generally underestimates average temperatures over Turkey. On one hand, the consistency of CCLM decreases up to -4℃ in the northeastern part of Turkey where high elevated mountains are located. On the other hand, over the Salt Lake in the central Anatolia region where the elevation is relatively low, the temperature biases are close to zero. The results indicate that the model estimates drift from the observations especially over the regions of steep topographical variations. For example, the annual temperature biases are low over Erzurum-Kars plato as well.

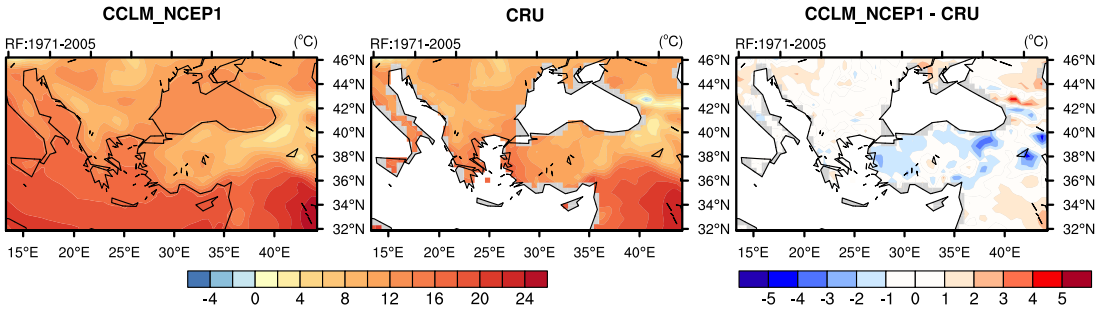

Figure 3.1 : Annual averages and bias of 0.44° CCLM_NCEP1 2-m temperature with respect to CRU data between 1971-2005 period.

Figure 3.2 illustrates the standard deviation of mean temperature of the CCLM_NCEP1 model and CRU, and also their difference over the domain between 1971 and 2005. It is obvious that the variability of annual cycle for the model is similar to the CRU observations. It appears that the standard deviation enlarges from the west to the east of Turkey and from the east of Turkey to Iraq. When the difference between standard deviations of the model and CRU is calculated, it is clearly seen that the standard deviation of the model is relatively lower over the Caucasus Mountains, the northeastern part of Turkey and Lebanon. This implies that the monthly temperatures oscillate around the mean more frequent compared to observations. On the contrary, the standard deviation of the model is approximately 1℃ larger than CRU over the rest of Turkey and Europe. Due to the large spatial variability of the mean seasonal model bias over most part of Europe and Turkey, overestimation of spatial temperature variability by CCLM_NCEP1 stands out from other regions.

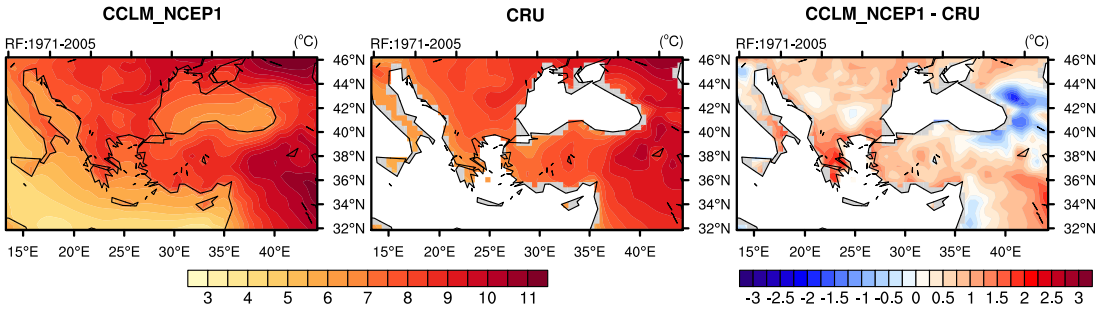

Figure 3.2 : Standard deviation and bias of 0.44° CCLM_NCEP1 2-m temperature with respect to CRU data between 1971-2005 period.

When the seasonal averages are analyzed, it is seen that CCLM_NCEP1 mimics the pattern of temperature distribution quite well (Figure 3.3). The largest cold bias is observed in winter season. The European countries that have positive bias in summer season such as Italy and Greece experience generally negative bias in winter season.

When the relatively elevated regions are taken into consideration like North Anatolian Mountains (Pontic Mountains), nearly 3℃ lower temperatures are generated by CCLM_NCEP1 for all seasons in comparison with CRU temperatures. CRU gridded data is produced by interpolation of near-surface observation stations. Therefore, the values over Turkey correspond to observation network of TSMS. When the distribution of meteorological stations in Turkey is taken into account, it is seen that the stations are located at fairly low elevations. That is why representation problem of mountainous regions occurs in gridded datasets. In other words, interpolated temperature values in highly elevated regions are warmer than the actual observation values. This situation causes the cold bias of the model to be seen higher in the model simulations. For the Aegean Region, CCLM_NCEP1 simulates colder than the observations in three seasons but closer values (±1℃) to the observations in summer.

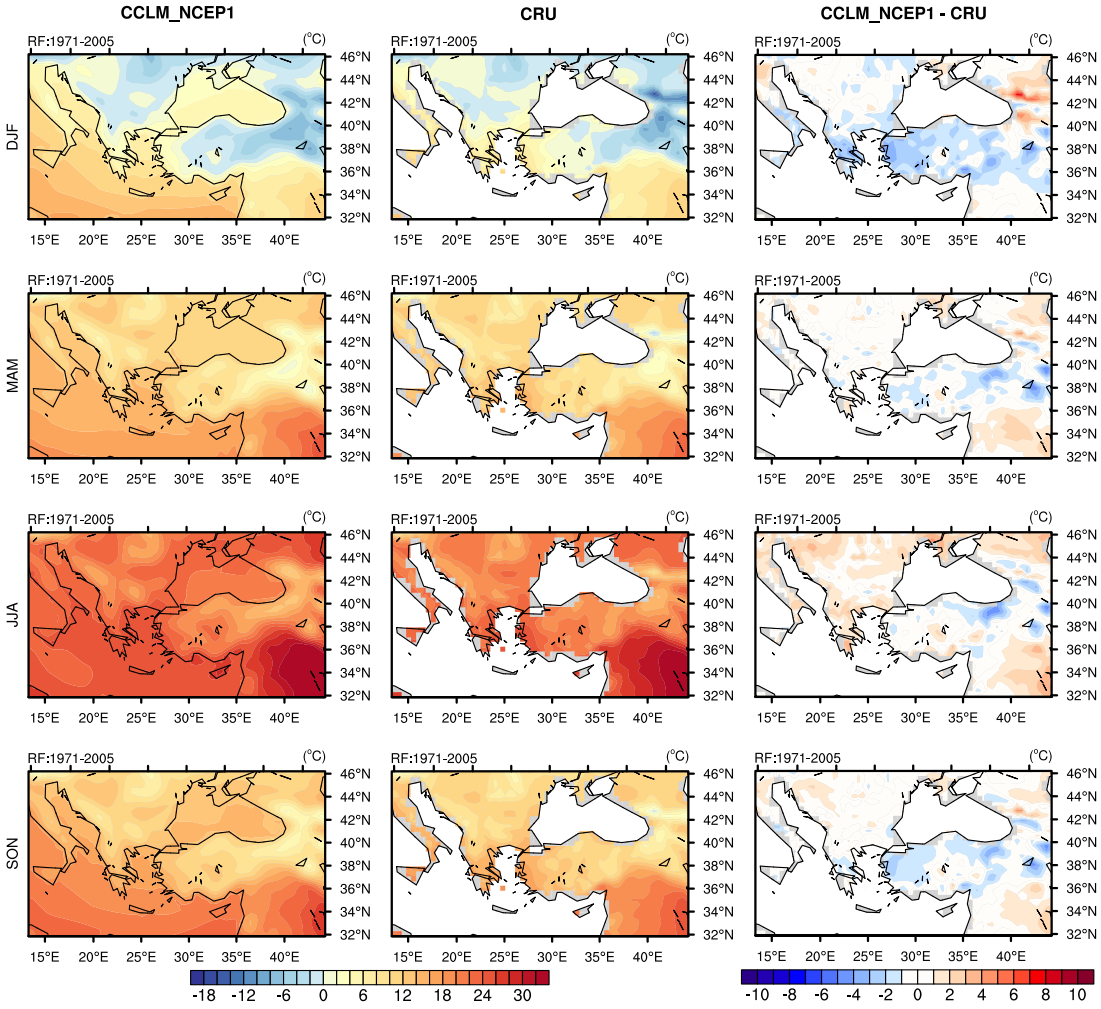

Figure 3.3 : Seasonal averages and biases of 0.44° CCLM_NCEP1 2-m temperature with respect to CRU data between 1971-2005 period.

3.1.1.2 Precipitation

The consistency of the precipitation with respect to observations depends on the horizontal and vertical resolutions of the model, PBL parameterizations, microphysics parameterizations and coupled ocean, land biosphere models. Therefore, it is a challenging task in modelling. Figure 3.4 shows the distribution of annual total precipitation simulated by the CCLM regional climate model and by CRU between 1971-2005 and the difference of CCLM from CRU. The most pronounced features are summarized as follows. Croatia's coastal region along the Adriatic Sea receives around 1400 mm annual precipitation according to CRU data. However, the CCLM_NCEP1 model estimates total annual precipitation in this region below 1000 mm. Similarly, CCLM_NCEP1 reveals negative anomalies over Romania and Slovenia compared to CRU. The underestimation of precipitation over Slovenia exceeds -800 mm. The model produces very close values to the precipitation observations of CRU over centeral and eastern Turkey and also over Bulgaria. Generally, the CCLM_NCEP1 shows a tendency of producing less precipitation especially on the western borders of the land areas if there exist topographical bariers.

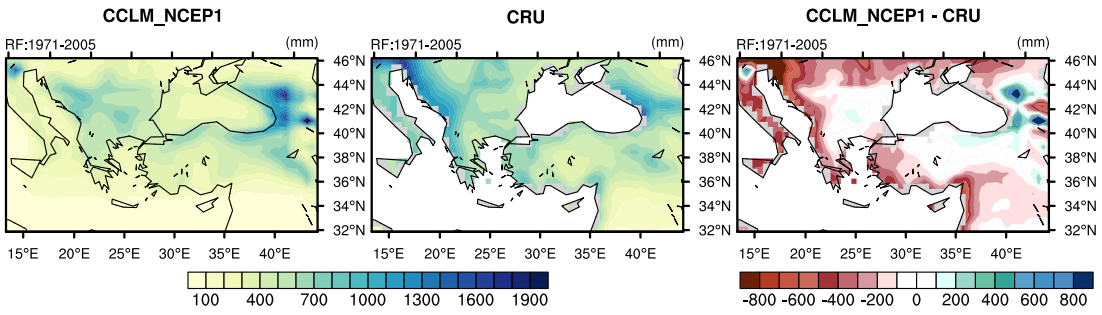

Figure 3.4 : Annual sums and bias of 0.44° CCLM_NCEP1 total precipitation with respect to CRU data between 1971-2005 period.

The standard deviations of the CCLM_NCEP1 model and CRU observation data, together with the difference between the two, are presented in Figure 3.5. The standard deviation of CCLM precipitation results is higher in eastern Turkey than in inner regions. The standard deviation of total precipitation around the Salt Lake (Central Anatolia) is also low for CRU observations. The variability in the annual rate of precipitation simulated by the model occurs in a broader range. The difference between winter and summer precipitation is high since the model predicts higher precipitation, especially in areas where elevation is high. Therefore, positive bias is

observed aroud Alpine and Caucasus regions with respect to CRU. Beguería et al. (2015) claims that the variance of a true field is systematically underrated and this bias gets larger if the sample size is reduced. Hence, these bias results could arise from the gridded data set.

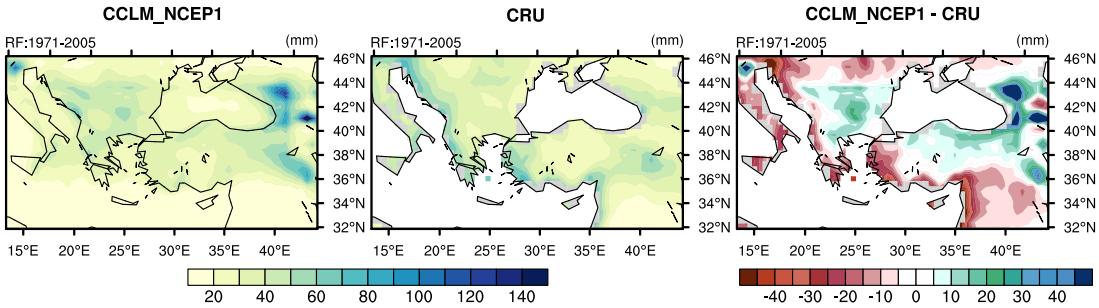

Figure 3.5 : Standard deviation and bias of 0.44° CCLM_NCEP1 total precipitation with respect to CRU data between 1971-2005 period.

In Figure 3.6, left column shows seasonal total precipitation distrubition simulated by CCLM_NCEP1, central column shows seasonal total precipitation distrubition provided by CRU and right column shows distribution of precipitation bias against CRU for the four seasons. In western Turkey, the seasonal bias in precipitation remains below -50 mm, except for the summer season. However, there are about 200 mm positive bias in the spring season on the mountainous regions such as Caucasus. However, the precipitation is always less over Italy in all seasons and this results in negative bias ranging between -100 and -200 mm. Only in the Alpine area, overestimation is observed in all seasons except for summer. Bucchignani et al. (2016) reported the same positive bias (in DJF) over the Alpine region of Italy in the ERA-Interim driven CCLM simulations and claimed that this can result from coarser resolution of orography, which causes overprediction of the precipitation on the leeside of the mountains. In addition to Italy, less precipitation is estimated particularly over the shorelines of Adriatic, Aegean and Mediterranean Sea with respect to CRU data for all seasons excluding summer. Due to low summer precipitation, the regional climate model has a high consistency in Syria, Iraq and Turkey in summer season. On the contrary, there is a strong underestimation of total precipitation during summer and the negative bias reaches up to -400 mm around Alps. Meanwhile, CCLM_NCEP1 simulates fairly well over Balkans in most of seasons.

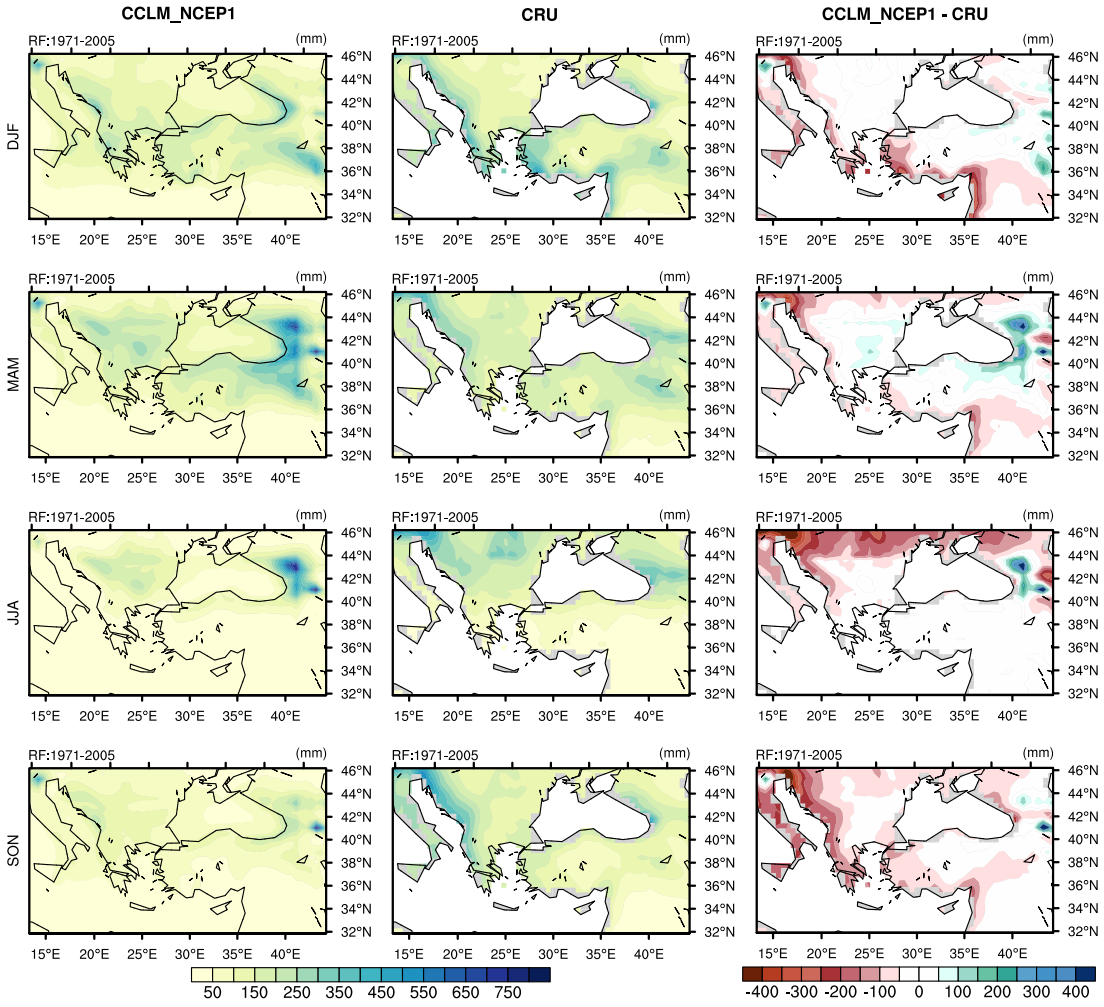

Figure 3.6 : Seasonal sums and biases of 0.44° CCLM_NCEP1 total precipitation with respect to CRU data between 1971-2005 period.

3.1.2 Evaluation of 0.11° simulations

In this section, simulations of the CCLM model forced with NCEP/NCAR Reanalysis 1 with 0.11° resolution for the 1971-2005 reference period were compared with the monthly average temperature and total precipitation values obtained from the TSMS stations on annual and seasonal basis. Since the global data sets does not meet the model resolution, and also the inner domain covers only the northwestern part of Turkey, the comparisons were done with the station observations. In order to make comparison between the model simulations and meteorological stations, simulated values at grids close to the station point were interpolated to station location using the bilinear interpolation method. In addition to geographical distribution of 35-year (1971-2005) annual and seasonal biases, contribution (in %) of seasonal to annual total precipitation over the stations in the study domain were calculated by dividing seasonal average to annual sum and

multiplying the result with 100. For average temperatures, an extra bias analysis was performed after the elevation correction had applied. The station heights were subtracted from the model heights (shown in Figure 3.7), and these values were added to the model outputs after being multiplied by the average lapse rate (6.5 °C/km), which expresses the change in temperature with height. Then, model consistency has been tested in the northwestern part of Turkey.

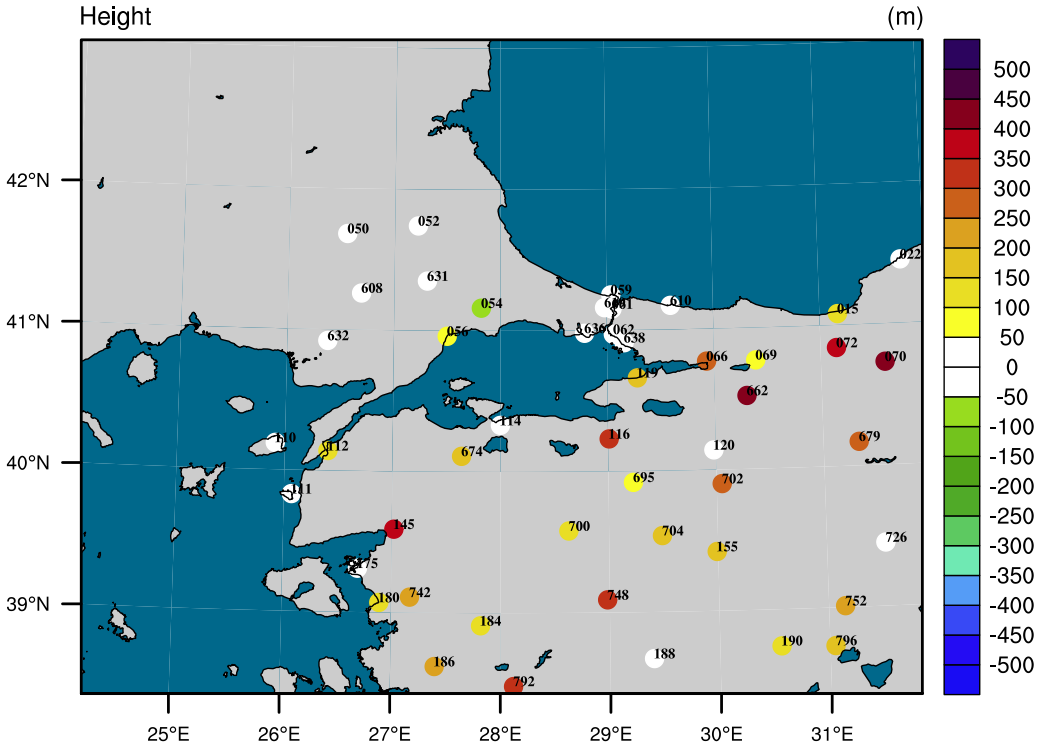

Figure 3.7 : The elevation difference between the CCLM model and TSMS stations. Last three digit of the station numbers are located on the points.

3.1.2.1 Temperature

The annual average temperature difference between the model and station values for the reference period of 1971-2005 are illustrated by Figure 3.8. According to 0.11° resolution results, the annual average temperatures differ between -4°C and 0.4°C from the station observations. This indicates that CCLM_NCEP1 has a tendency to underpredict mean temperatures according to station observations. However, the magnitude of the tendency is not that high because the average bias of all stations is -1.3°C. The model produces coldest temperatures where the model elevation at least 200 meters higher than station (Figure 3.9). That is why the average bias of all stations is approximated to -0.5°C after the model temperatures are corrected with respect to topography.

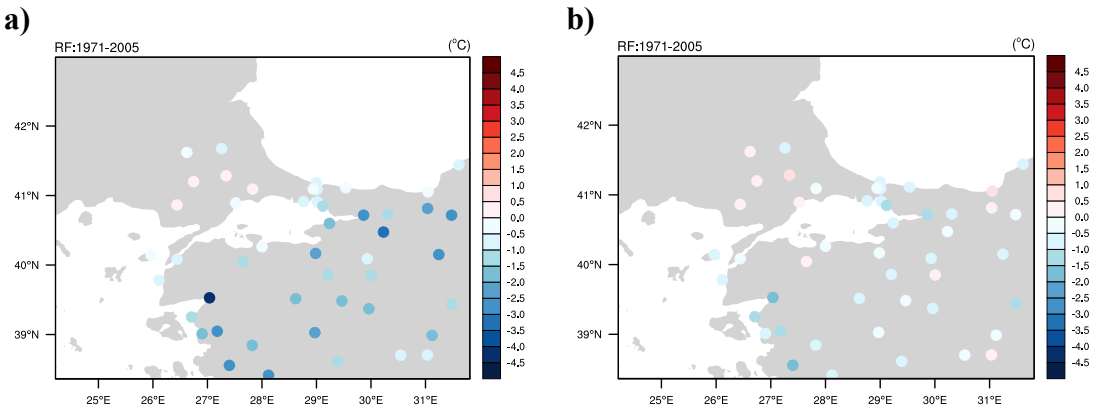

Figure 3.8 : a) Annual temperature bias and **b)** elevation corrected annual temperature bias of 0.11° CCLM_NCEP1 simulations with respect to TSMS observations for 1971-2005 reference period.

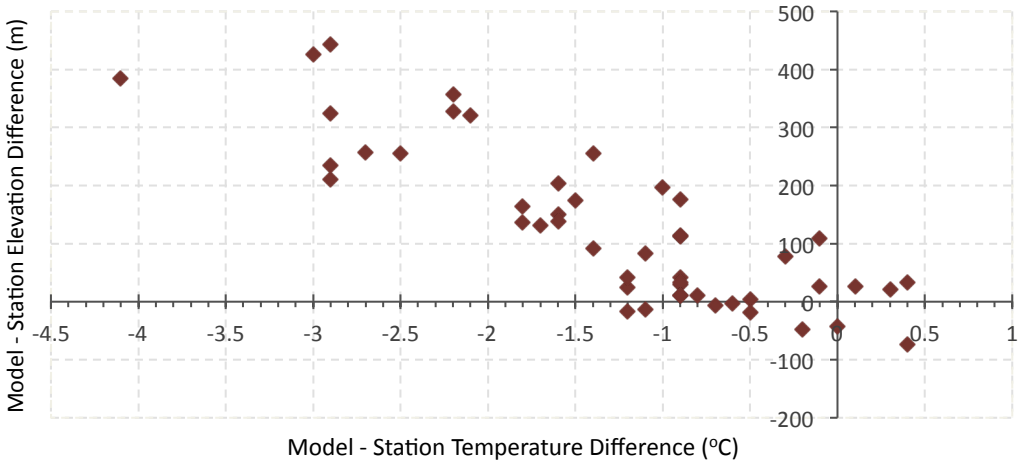

Figure 3.9 : The relation between the annual temperature bias (CCLM - TSMS) and elevation difference between model and meteorological stations.

The difference between the seasonal average of the simulation and station values for the monthly average temperature during the 1971-2005 reference period are given in Figure 3.10. In all seasons, model produces colder temperatures than observations especially for stations located at relatively higher elevation. This cold bias weakens after the elevation correction is applied. For instance, Edremit station numbered as 17145 (shortly 145), has higher negative anomaly than the other stations with a temperature difference above -5 ℃, which is decreased up to -3 ℃ after elevation correction. Since the Aegean Region has mostly negative anomaly values in all four seasons, it is understood that the CCLM model simulates lower average temperatures than observations (Figure 3.11-a) but after the elevation correction, this negative bias has been removed in all seasons, excluding winter (Figure 3.11-b). The temperature

bias averages on all station values were calculated as -2.7 ℃, -0.5 ℃, -0.4 ℃ and -1.5 ℃ in winter, spring, summer and autumn seasons, respectively. When the elevation correction is applied, the bias values approach to zero and new bias values are calculated as -1.9℃, 0.3℃, 0.4℃ and -0,7℃, respectively.

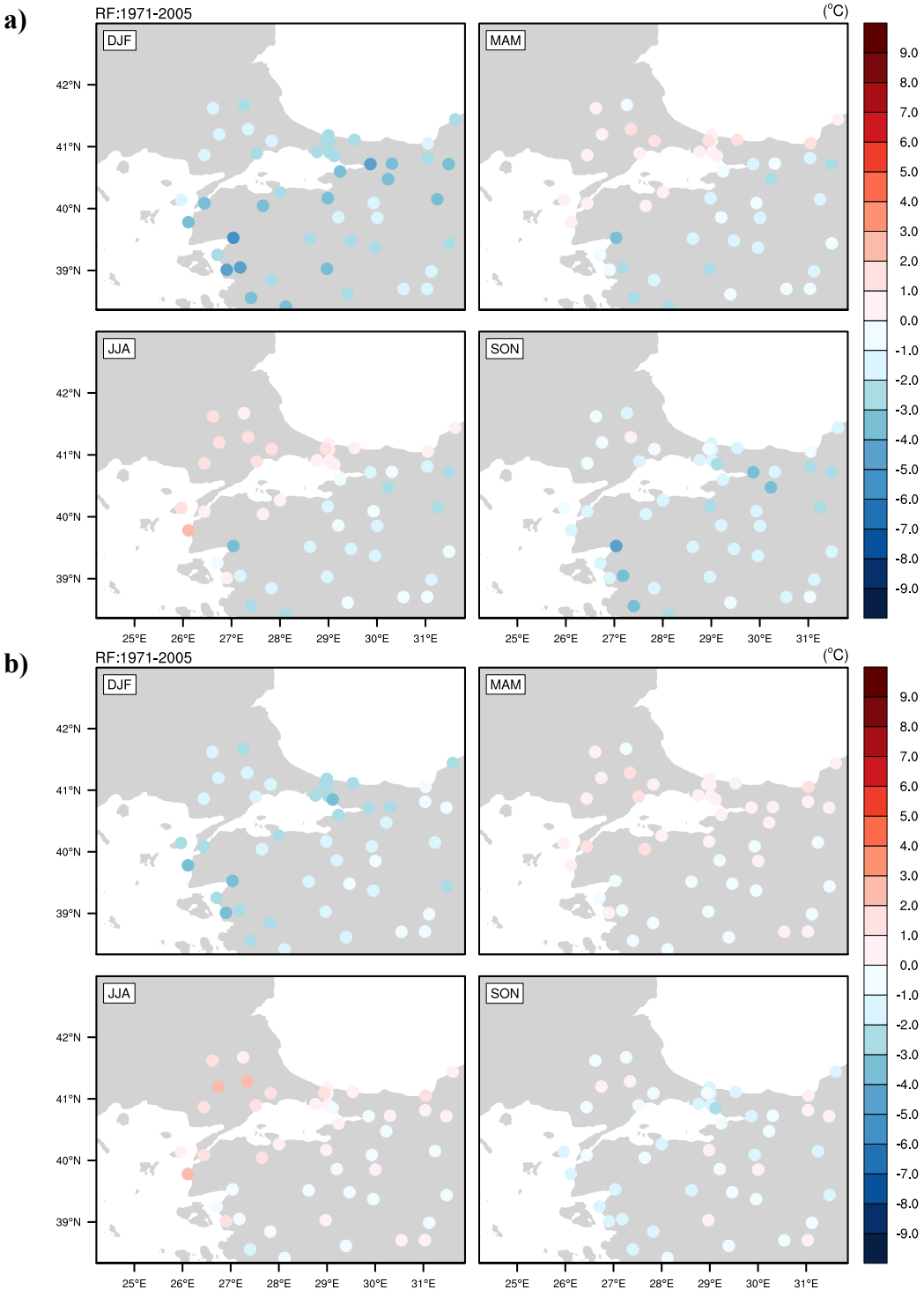

Figure 3.10 : a) Seasonal temperature biases, **b)** elevation corrected seasonal temperature biases of 0.11° CCLM simulations with respect to TSMS observations between 1971-2005 reference period.

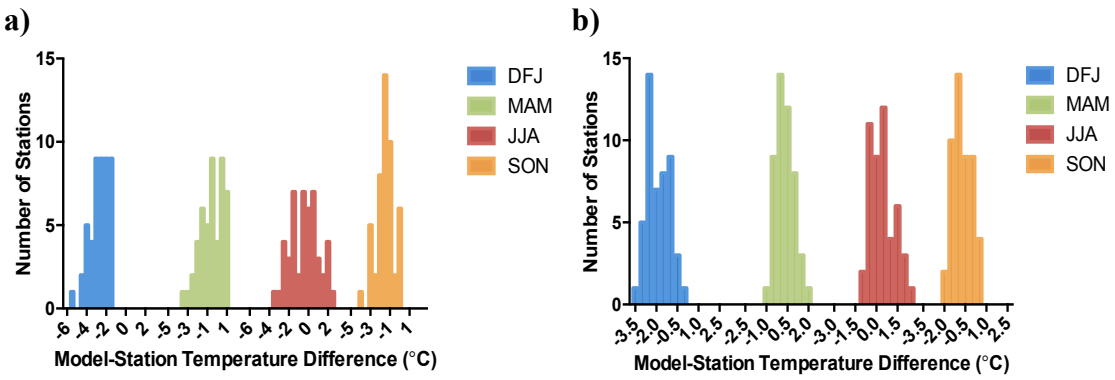

Figure 3.11 : The distribution of the seasonal temperature differences between the model at all station points and the TSMS observations.

3.1.2.2 Precipitation

The number of precipitation stations equal to the temperature stations. When the annaul average of total precipitation of the model is subtracted from station values, it is asserted that the model underestimates average -180.6 mm less precipitation than observations (Figure 3.12). The higher resolution results are consistent with the results of the lower resolution. The northern part of the model domain, which lies throughout Black Sea coast line, is dominated by negative biases. The maximum dry bias is observed in 17022 Zonguldak station with -737.3 mm. It is followed by 17619 Bahcekoy station with -625.4 mm. Meanwhile, the standard deviation of all points is calculated as 167,4 mm.

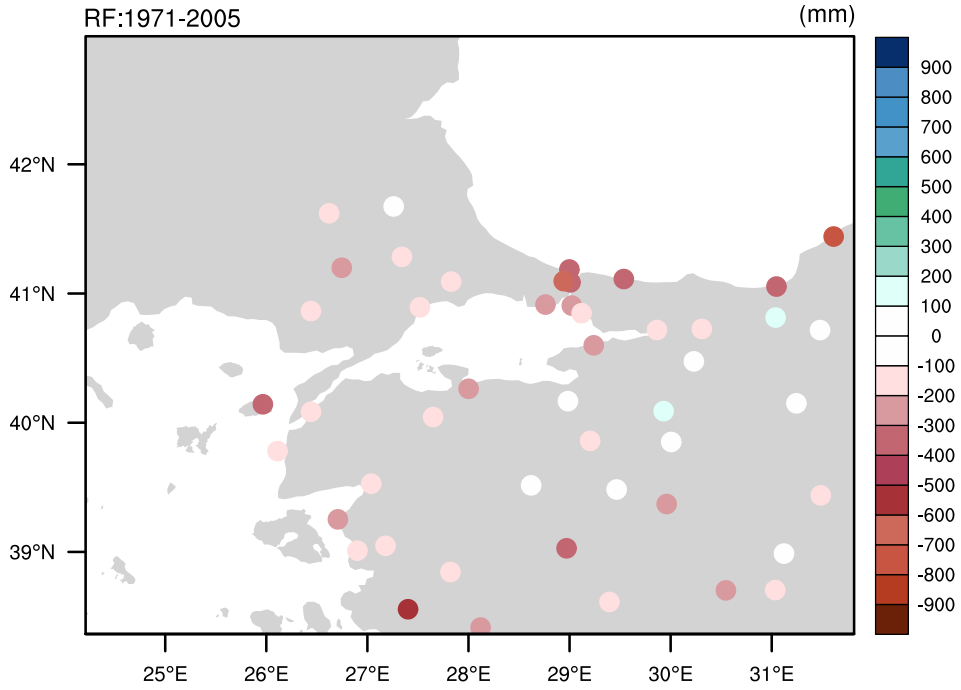

Figure 3.12 : Annual precipitation bias of 0.11° CCLM_NCEP1 simulations with respect to TSMS observations between 1971-2005 reference period.

The comparison of seasonal averages of total precipitation obtained from 48 stations with the CCLM_NCEP1 total precipitation simulations implies that the model produces less precipitation than observations, especially in winter and autumn (Figure 3.13). The averages of seasonal precipitation differences are computed as -71.3 mm in winter, 0.7 mm in spring, -16 mm in summer and -87.7 mm in autumn. Futhermore, seasonal standard deviations between stations' biases are above 40 mm except for the summer season. Error distributions are presented in Figure 3.14. The distributions of precipitation errors are similar in summer and spring seasons. For instance, the biases are close to zero at approximately 17 stations in spring season and summer comes after spring with nearly 15 stations. Extreme bias values are detected mostly in the autumn season. The biases exceed -80 mm at several meteorological stations, and what is more the biases are skewed left which shows the mean is smaller than the median. It should be noted that model simulations correspond to areal values over approximately 12x12 km^2 whereas station values are provided from point observations. Beside these, the model is usually more sensitive over central region of Turkey.

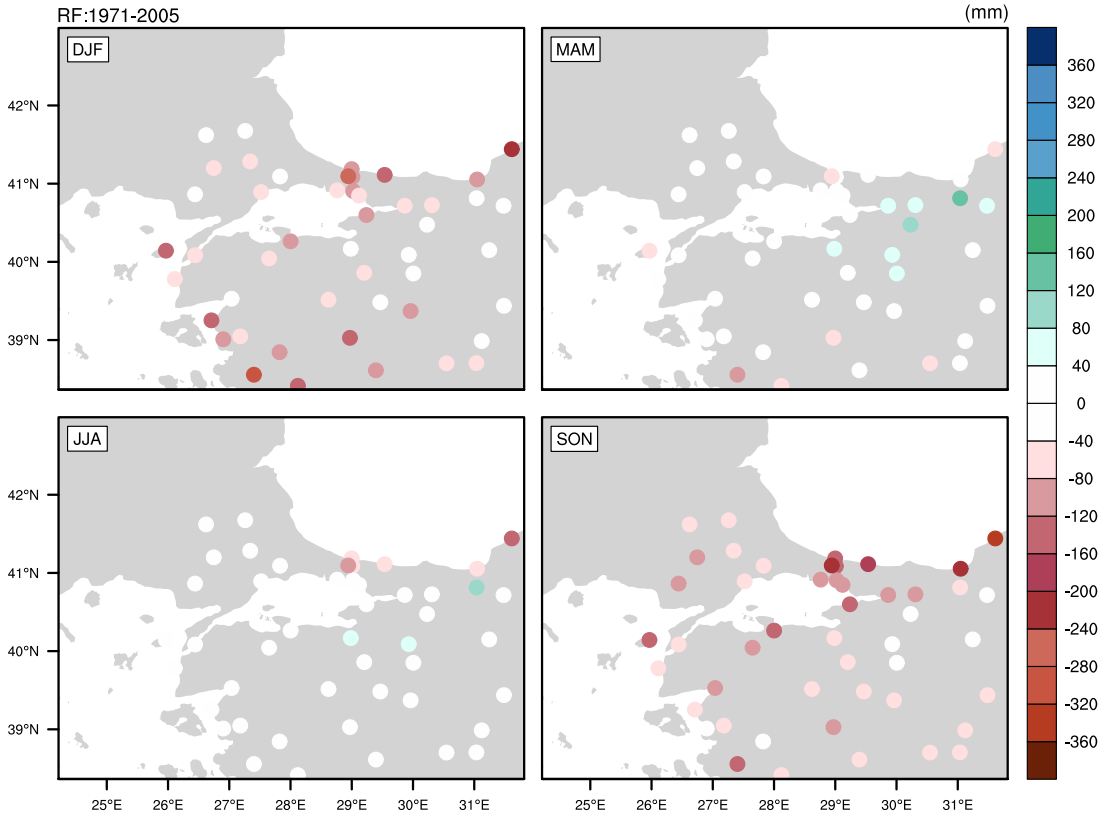

Figure 3.13 : Seasonal total precipitation biases of 0.11° CCLM_NCEP1 simulations with respect to TSMS observations between 1971-2005 reference period.

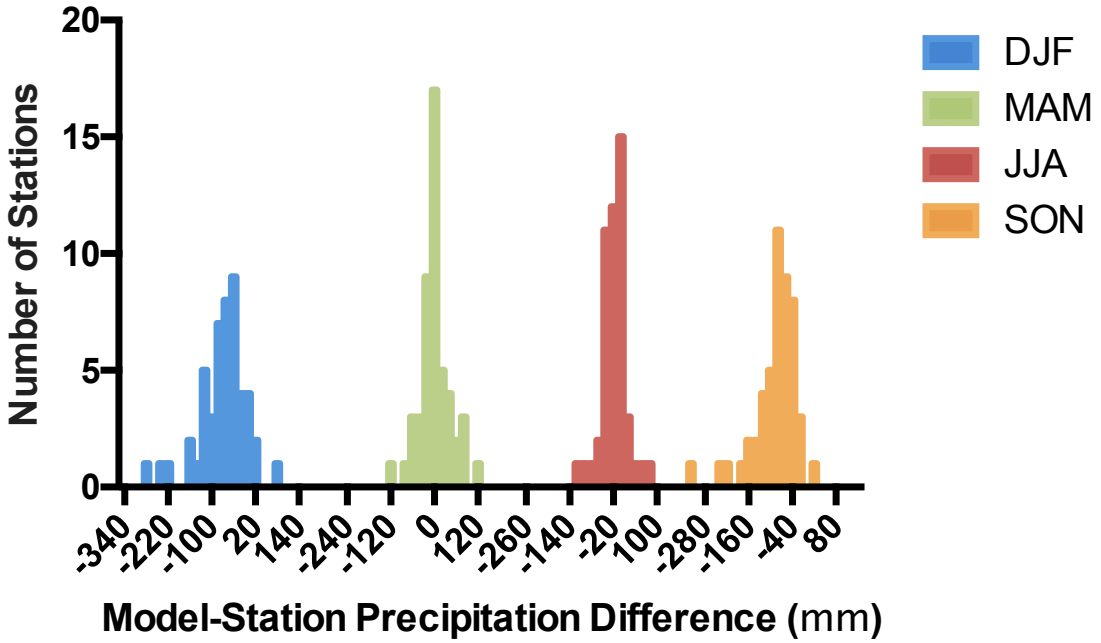

Figure 3.14 : The distribution of the seasonal total precipitation differences between the CCLM_NCEP1 model at all station points and the TSMS observations.

The spatial distribution of 35-year contribution of seasonal total precipitation to annual total precipitation is given in Figure 3.15. The largest contribution to annual amounts is observed in winter season for both station observations and CCLM_NCEP1 simulations. Hatzianastassiou et al. (2016) claim that the highest winter contribution to annual totals results from cyclonic activity that causes substantial precipitation amounts and dominates Mediterranean region chiefly during winter season. The contribution of winter, which is calculated from TSMS observations (Figure 3.15-a), ranges from 25% to 50% all over the domain while the contribution of simulated winter (Figure 3.15-b) changes between 20% and 50%. However, the model catches the contribution pattern quite well for winter and summer, exlcuding Aegean Region. The contribution of other seasons do not surpass 35% except for spring season of CCLM_NCEP1 simulation. In TSMS observations, the percentage of spring contribution ranges between 15 and 35. On one hand, the simulated spring season (Figure 3.15-b) contribute nearly 10% more than observed spring season (Figure 3.15-a) to the annual total precipitation almost all over the study region. The contribution percentage exceeds 40 over central Turkey during spring of CCLM_NCEP1. On the other hand, the simulated autumn season contribute to annaul amounts 5-10% less than observed autumn season and the distinctive difference comes up along the Black Sea coast line and around central Turkey.

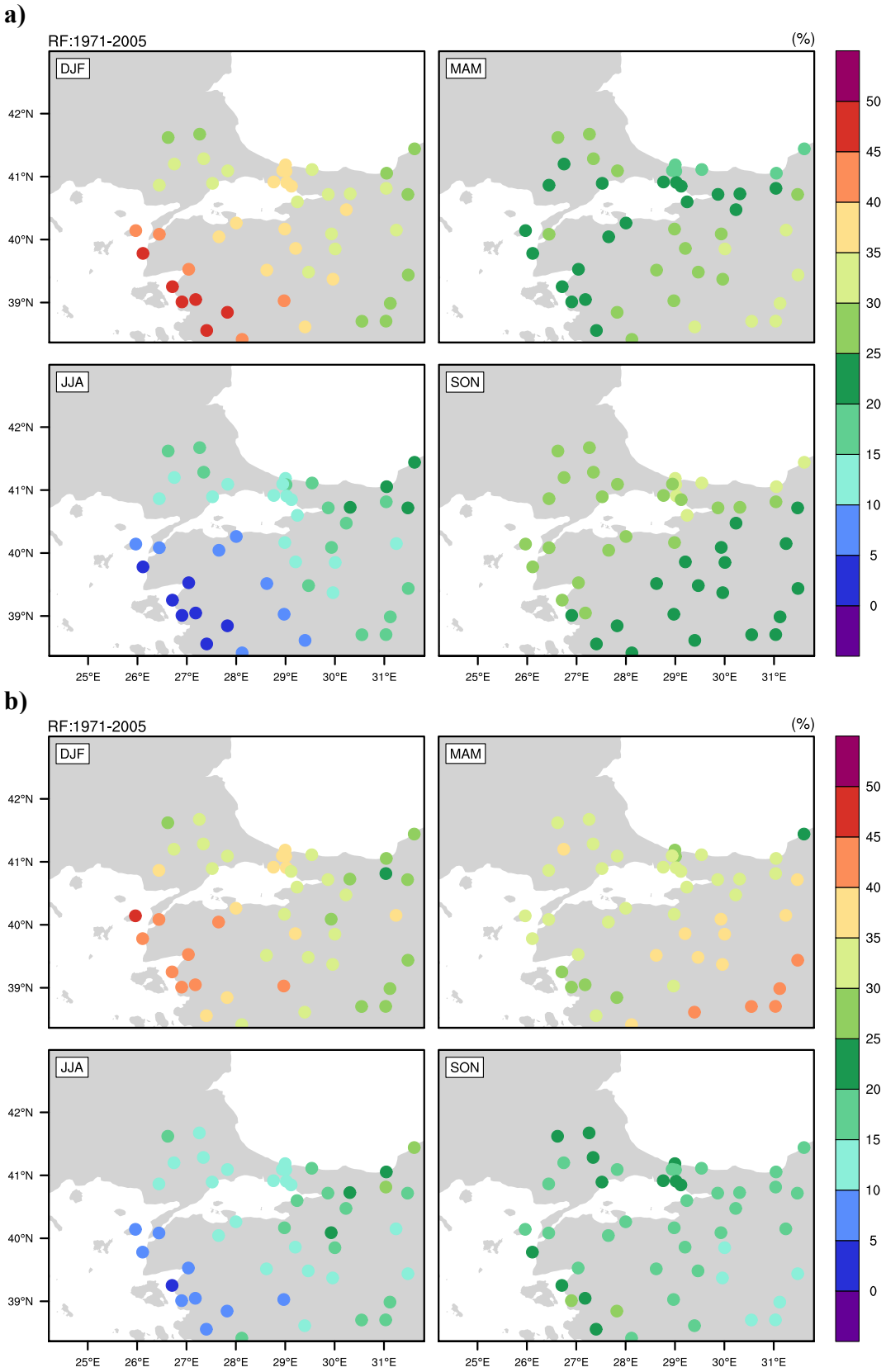

Figure 3.15 : Contribution of seasonal to annual total precipitation calculated from **a)** TSMS stations, **b)** 0.11° CCLM_NCEP1 simulations for 1971-2005 reference period.

3.2 Downscaling Earth System Model Simulations

3.2.1 Evaluation of 0.44° simulations

In addition to evaluation with NCAR/NCEP Reanalysis data, the CCLM model is also forced with MPI-ESM-LR earth system model outputs for 0.44° resolution in order to explore how much is the total bias of the CCLM coupled with MPI-ESM-LR since the one of the purposes of this thesis is to explore the future changes in surface climate variables under RCP8.5 scenario. Mother domain results are compared with CRU data that is bilineerly interpolated to the model grids. The rows named as "DJF", "MAM", "JJA" and "SON" in the figures represent winter, spring, summer and fall seasons, respectively.

3.2.1.1 Temperature

The annual average temperature distribution of CCLM_MPI-ESM-LR simulation and CRU observation data between 1971-2005 and their differences are given in Figure 3.16 while their standard deviations are shown in Figure 3.17. As can be moved from west to east of Turkey, both the model and CRU temperatures show decreasing tendency which demonstrates the strong influence of elevation in the model. In the southern part of domain, specifically over Iraq, the temperature appears higher compared to other regions but CCLM_MPI-ESM-LR simulates mean temperature approximately 3℃ higher than CRU. However, the maximum bias is not seen over this region. On the contrary, positive bias exceeds 4℃ over Caucasus Mountains. The model generates mostly consistent temperatures over Europe and also over Turkey with ±2℃ annual temperature bias. In the central Anatolia region where the elevation is relatively low, the temperature biases are close to zero. But over the western Turkey, the negative bias increases up to -2℃. The distribution of the biases are very similar to the one forced by NCEP reanalysis data except where the nort-eastern and south-eastern latitudes of the domain have slightly higher temperature biases. On the other hand, the biases along the Black Sea coast are confined between -1℃ and +1 ℃. And the coupled system shows less temperature biases over Turkey compared to CCLM forced by reanalysis.

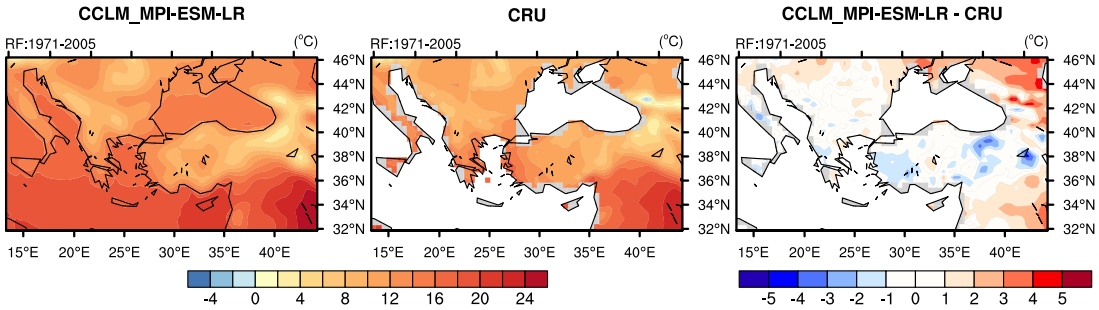

Figure 3.16 : Annual averages and bias of 0.44° CCLM_MPI-ESM-LR 2-m temperature with respect to CRU data between 1971-2005 period.

As can be construed from Figure 3.17, the standard deviation pattern of CCLM_MPI-ESM-LR is very similar to CRU observations. In both, standard deviation increases from the west to the east of Turkey and the highest deviations from the mean are seen over Russia, the region above Caucasus Mountains. The model has a tendency to estimate temperature values around the mean more frequent than the CRU values. The negative peak values based on the standard deviation difference between the model and CRU are observed over elevated regions such as Caucasus Mountains. On the contrary, the difference is only high over Iraq and the southern coastal region of Turkey. The results reveal that the seasonal and interannual variability of the coupled system is lower than the simulations of CCLM forced by NCEP reanalysis data in almost everywhere of the domain.

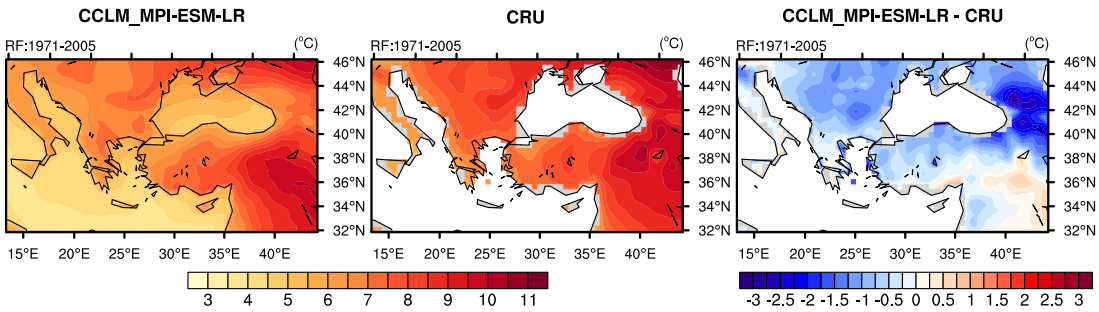

Figure 3.17 : Standard deviation and bias of 0.44° CCLM_MPI-ESM-LR 2-m temperature with respect to CRU data between 1971-2005 period.

The seasonal averages of the model and CRU temperatures are illustrated by Figure 3.18. The CCLM_MPI-ESM-LR model captures the mean temperature pattern well according to CRU observations. The topography of the domain can be easily understood from the temperature distribution throughout the domain. Since the temperaure has inverse relation with altitude, elevated regions display cooler temperatures relative to other regions. For both, boreal summer temperatures reach up to 32℃ over Iraq while winter temperatures decrease up to -8℃ over

eastern/northeastern Turkey, Caucasus Mountains and Transylvanian Alps. However, the model generally overestimates the mean temperature over Caucasus Mountains and the bias exceeds to 8℃ in winter. Especially in winter and fall seasons, the model projects very similar temperatures to CRU over Turkey. On the contrary, most of the European countries experience warmer temperatures during these seasons in comparison to CRU. Furtermore, the model generates colder temperatures over Turkey in spring and summer. The average temperature biases for spring and summer seasons reach to -4℃. It is clear that the CCLM has a cold bias in winter (Figure 3.3). However, when it is coupled with MPI-ESM-LR, the winter temperature biases change from negative to positive and they are quite low over Turkey. There is an improvement in the simulations of the present day average temperatures except summer season. Summer season is slightly colder than CCLM_NCEP1 temperatures.

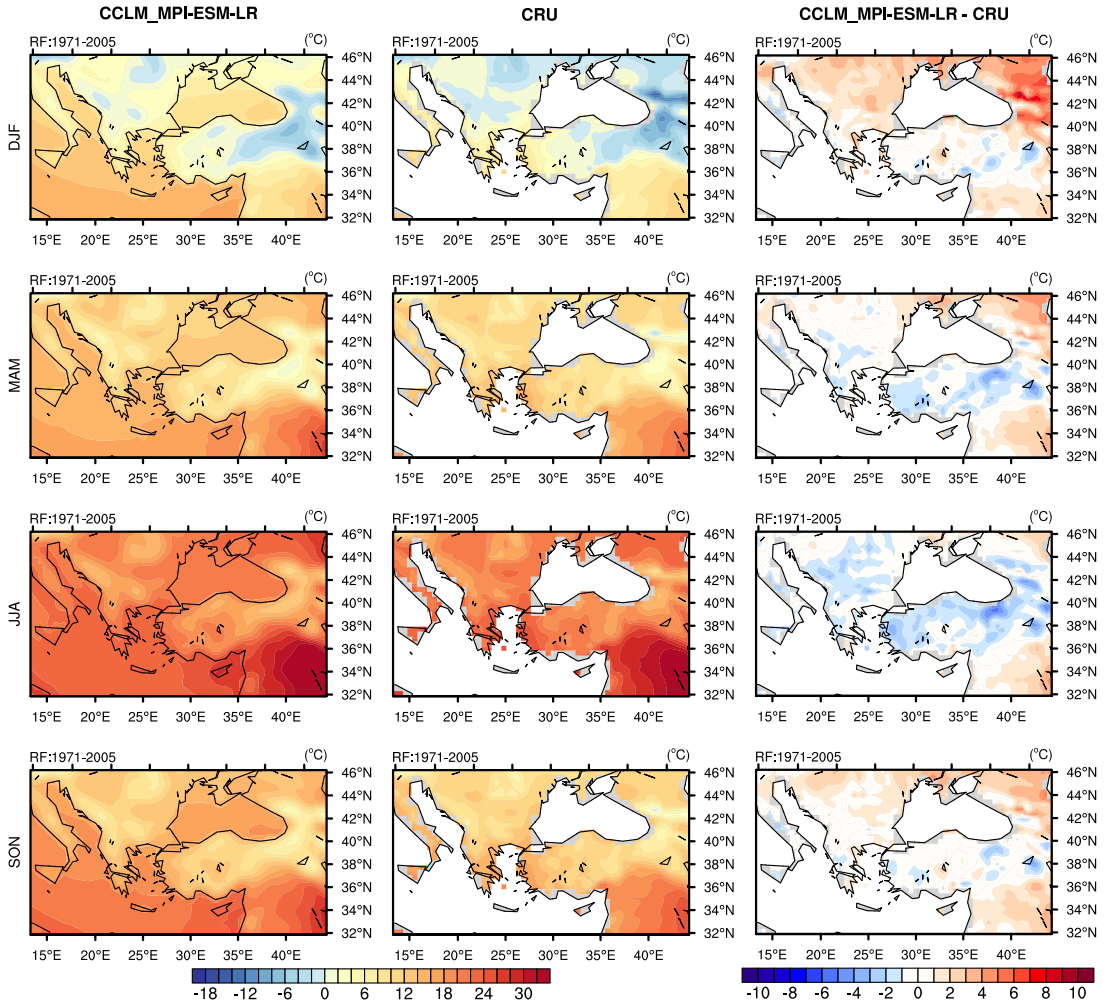

Figure 3.18 : Seasonal averages and biases of 0.44° CCLM_MPI-ESM-LR 2-m temperature with respect to CRU data between 1971-2005 period.

3.2.1.2 Precipitation

The annual total precipitation distrubitions of CCLM_MPI-ESM-LR (left column) and CRU (central column) and also the bias (right column) are evaluated for the period of 1971-2005 (Figure 3.19). On one hand, the model produces excesive amount of precipitation (>1900 mm) over Montenegro's coastal region along the Adriatic Sea but less precipitation is observed in CRU data, which leads to approximately 600 mm bias over that region. In addition to Montenegro, the precipitation becomes more intense also over Caucasus Mountains and northeastern part of Turkey and these regions are dominated by lowest consistency with 800 mm bias. On the other hand, less precipitation is simulated over Slovenia with respect to CRU observations and the magnitude of the reduction reaches to -600 mm. Meanwhile, the model is usually more sensitive over Syria. In general, MPI-ESM-LR produces more precipitation over Europe. From the section 3.1.1.2, it is seen that the CCLM has a tendency to produce less precipitation within the study domain. Since the coupling sytem are controlled by the MPI-ESM-LR earth system model, the biases of the coupled system are reversed. The combined model system are wetter than the observations.

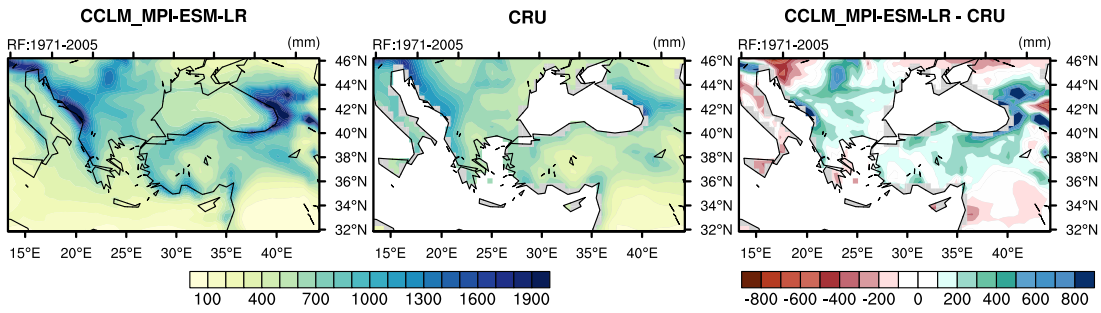

Figure 3.19 : Annual sum and bias of 0.44° CCLM_MPI-ESM-LR total precipitation with respect to CRU data between 1971-2005 period.

According to both the model and observation results, the standard deviation over the coastal regions along the Adriatic Sea and Aegean Sea is excessive (Figure 3.20). Furhermore, high standard deviations are estimated from the model results over the region of Alps, Caucasus, Southeastern Taurus and Hakkari Mountains. When the model is compared with CRU data, it is clearly seen that the CRU observations follow also similar pattern but the variation is considerably less than the model. The oscillation around the mean is higher in the model results. The seasonal and interannual variability of the precipitation are increased in the coupled system over

the western coast of the land areas in which COSMO_NCEP1 produced significantly less variability compared to CRU observations.

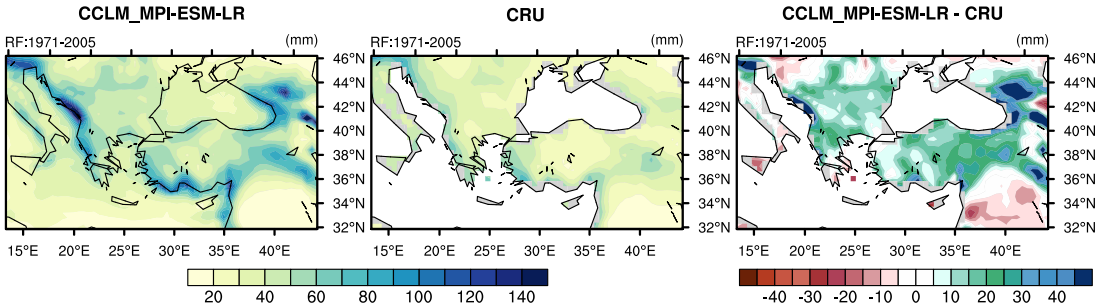

Figure 3.20 : Standard deviation and bias of 0.44° CCLM_MPI-ESM-LR total precipitation with respect to CRU data between 1971-2005 period.

The comparison of observations with the model simulations forced with the earth system model MPI-ESM-LR on a seasonal basis is shown in Figure 3.21 for the reference period of 1971-2005.

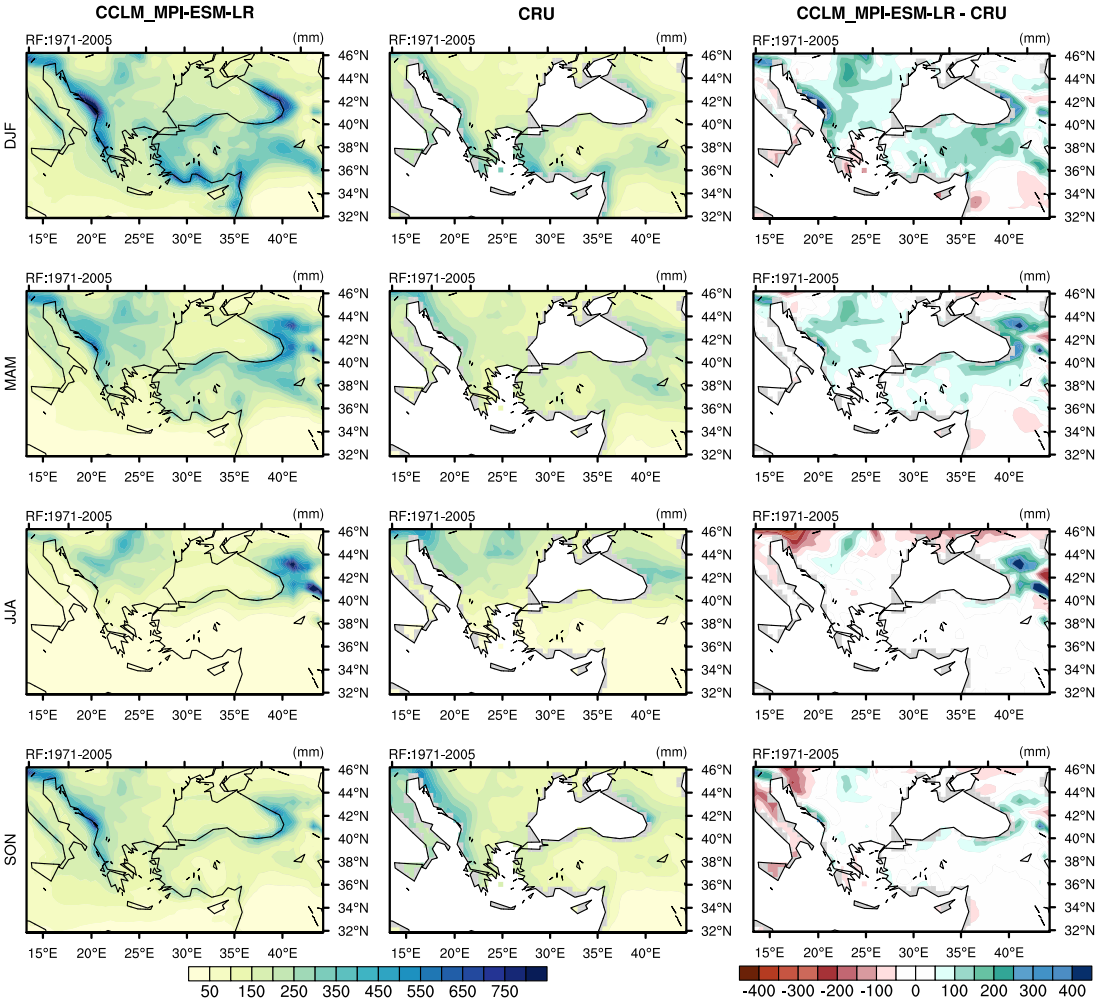

Figure 3.21 : Seasonal sums and biases of 0.44° CCLM_MPI-ESM-LR total precipitation with respect to CRU data between 1971-2005 period.

It presents that the coastal regions along the Adriatic Sea and the regions around Caucasus Mountains and Carpathian Mountains receive more precipitation in almost all seasons. Similar to the annual averages, the coastal area of Montenegro along the Adriatic Sea is exposed to more than 800 mm precipitation, especially during the winter but the same excessive precipitation is not observed in CRU data. In the Alpine region of Italy, the total precipitation is overestimated in all seasons except for summer. The same situation is also observed in NCEP1 driven simulations but the negative bias over the rest of Italy dissappers in the CCLM_MPI-ESM-LR. Mostly, the precipitation is overpredicted in the northeastern part of Turkey because of steep mountain barriers along the Black Sea. On one hand, CCLM driven by MPI-ESM-LR produces considerably high precipitation (>50 mm) compared to CRU values over Europe in winter and spring season. On the other hand, it predicts consistent precipitaiton values over Europe in the summer and autumn. The model simulations over Turkey reveal a more rainy climate during the winter and spring seasons whereas show high consistency with CRU data during the summer and fall seasons.

3.2.2 Evaluation of 0.11° simulations

Because of increasing the model resolution to 0.11°, the CCLM model simulations driven by MPI-ESM-LR were compared with the 2-m temperature and total precipitation taken from the TSMS stations. The nearest model grids to the observation coordinates were taken into consideration by reason of verifying the model simulations. Hereby, the bias of the model simulations was calculated for 48 point over northwestern Turkey by subtracting the observations from the model simulations. In order to reduce the topography effects on biases, the elevation correction method was applied to the temperature model outputs as it explained in the section 3.1.2 . Since the nested resolution of CCLM_MPI-ESM-LR and CCLM_NCEP1 are the same, elevation difference between the model and TSMS stations gives the same values (shown in Figure 3.7). The rows named "DJF", "MAM", "JJA" and "SON" in the figures represent winter, spring, summer and autumn seasons, respectively.

3.2.2.1 Temperature

The annual uncorrected and corrected temperature biases of the model with respect to 48 TSMS stations are presented in Figure 3.22 for the period of 1971-2005. The model produces warmer temperatures than observations particularly over northern part of the domain while generates colder values over southern parts. Nevertheless, the annual biases are commonly negative sided and ranges between -3.6℃ and 1.6℃ (Figure 3.22-a). It is noticable that the negative biases are mostly dominant over highly-elevated regions. For this reason, elevation corrected temperature biases are computed and average bias of all points is reduced from -0.49℃ to 0.3℃ in magnitude. Although the amount of the decrease is not that high, standard deviation of all points is lessened more. This implies that the simulated temperatures at the station points gets closer to the mean after elevation correction (Figure 3.22-b). When the elevation correction is applied to 17145 Edremit station that is nearly 385 meters lower than model height, the extreme cold bias is reduced from -3.6℃ to -1℃. Another example is 17111 Bozcaada station which is located at approximately the same height with the model height. The bias at Bozcaada station (0.2℃) does not change after elevation correction. These are good examples to show that the negative bias strengthens as the discrepancy between the model topography and real topography increases (Figure 3.23). Meanwhile, the biases along the coast line do not change substantially since the elevation difference between the model and stations is not that high.

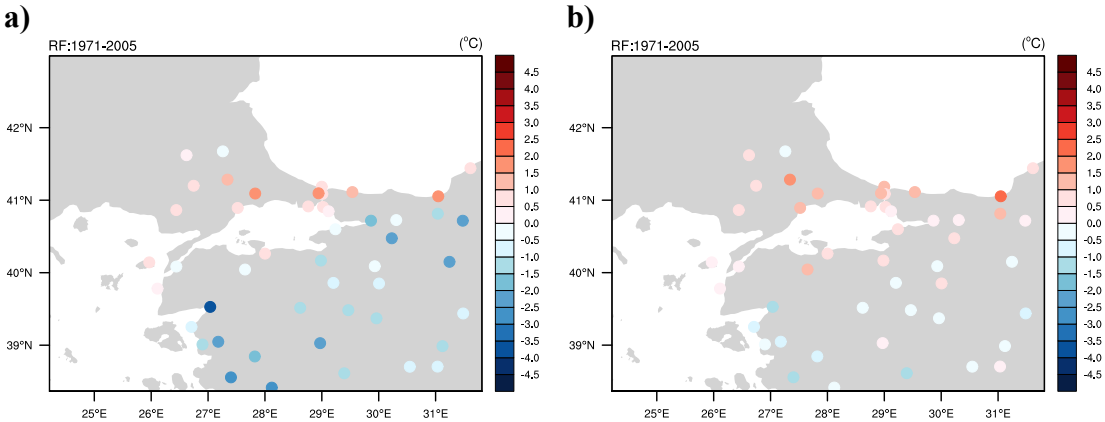

Figure 3.22 : Annual temperature **a)** biases, **b)** elevation corrected biases of 0.11° CCLM_MPI-ESM-LR simulations with respect to TSMS observations between 1971-2005 period.

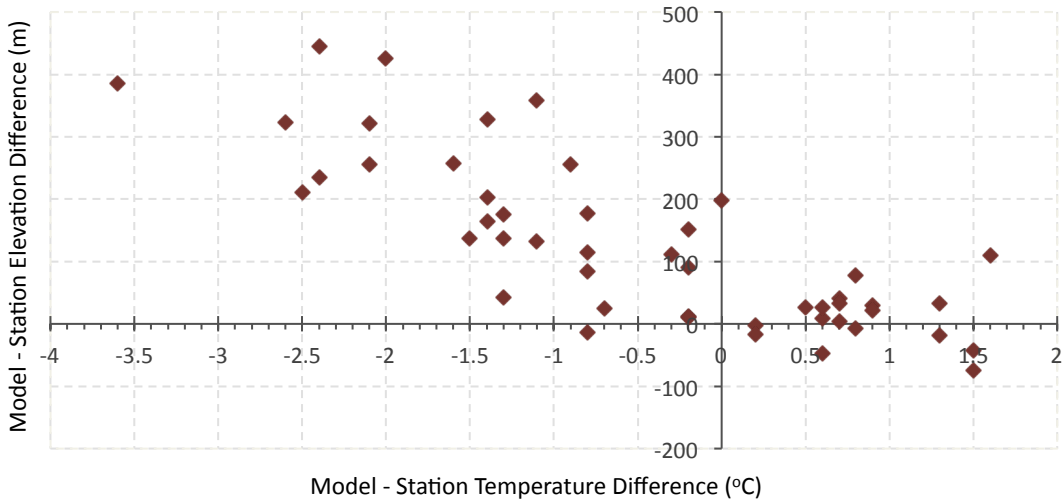

Figure 3.23 : The relation between the annual temperature bias (CCLM - TSMS) and elevation difference between model and meteorological stations.

When the calculated seasonal biases for mean temperature are visualized by ignoring the effect of topography first, the average model-observation bias is calculated approximately -4℃ in the summer season for Aegean region where the altitude is relatively high while the lowest bias values are estimated around -1.3℃ for winter season but in general the CCLM_MPI-ESM-LR model has negative biases along the Aegean coastline (Figure 3.24-a). After the elevation correction, the average summer bias over Aegean stations (including Edremit, Dikili, Akhisar, Manisa, Bergama, Salihli) is reduced to -2.5℃ whereas the average winter bias over the same stations is shifted to 0.3℃ (Figure 3.24-b). In contrast to Aegean stations, the coupled model system usually has positive bias over Black Sea coast line especially in winter and spring seasons. Additionally, summer has the coldest biases reaching up to -5℃ within all seasons that is shown in Figure 3.25-a. Extreme bias values are observed in all seasons yet the variation range of temperature difference becomes narrow when the biases are corrected with respect to elevation (Figure 3.25-b). For instance, the variation range of autumn ranges between -3℃ and 2℃. It changes between -0.8℃ and 2.7℃ after elevation correction. This case is valid also for most of seasons. The standard deviations of all stations located in the whole domain were calculated as 1.2 ℃, 1.5 ℃, 1.4 ℃ and 1.1 ℃ for winter, spring, summer and autumn seasons, respectively. When the elevation correction is exerted, the standard deviations are decreased to 0.7℃, 1.0℃, 0.9℃ and 0,7℃, respectively. Nevertheless, the outcome

of the bias averages on all station values does not reveal the efficiency of the elevation correction for each season.

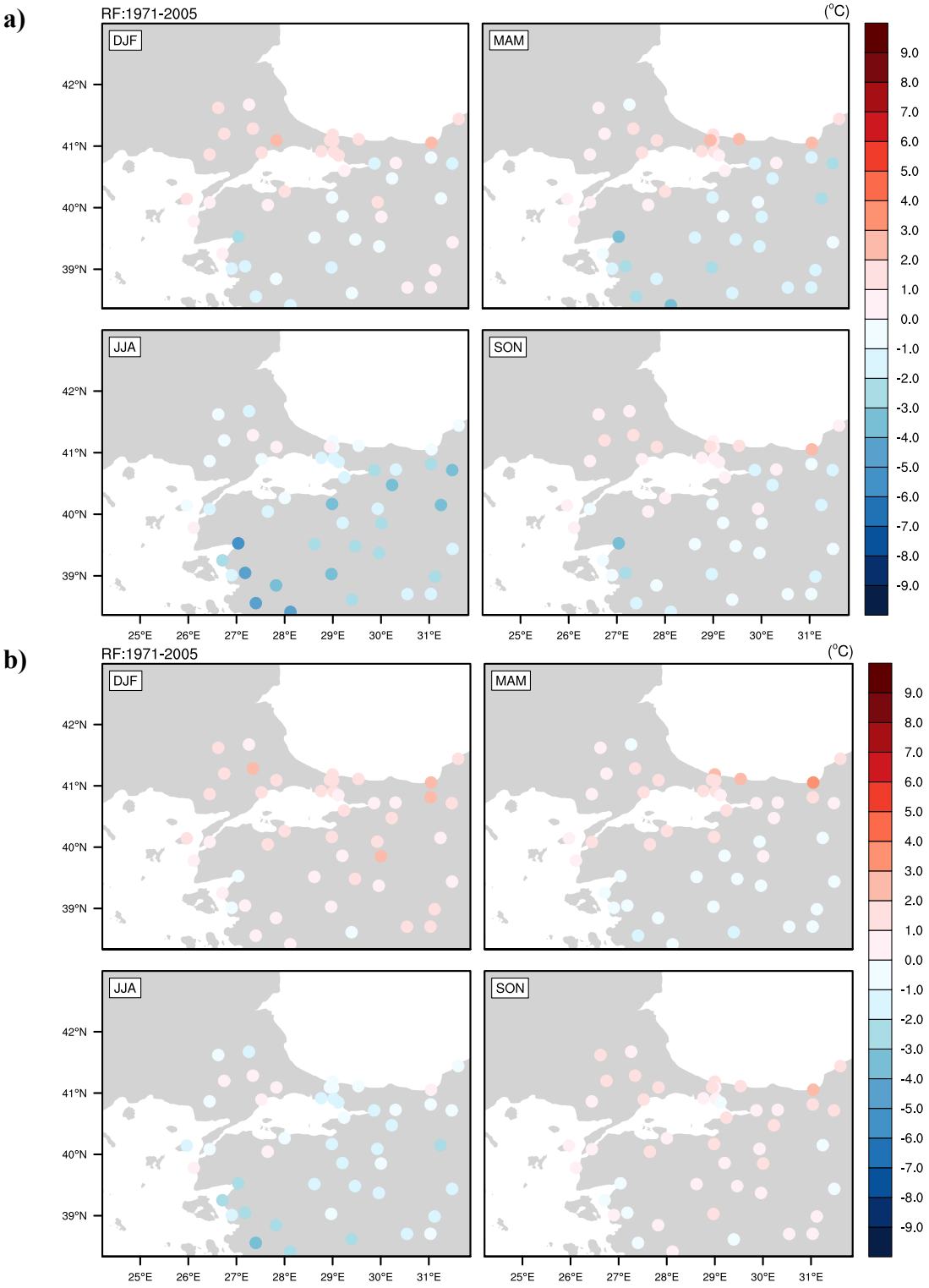

Figure 3.24 : Seasonal temperature **a)** biases, **b)** elevation corrected biases of 0.11° CCLM_MPI-ESM-LR simulations with respect to TSMS observations between 1971-2005 period.

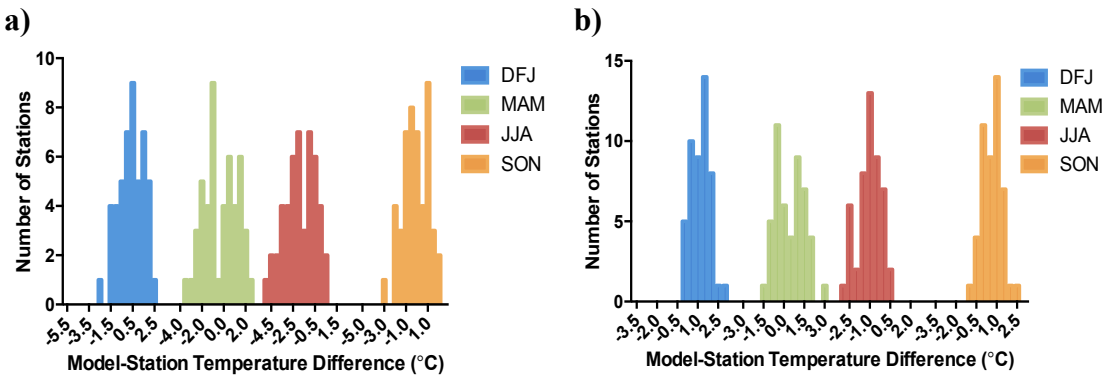

Figure 3.25 : The distribution of the seasonal temperature differences between the CCLM_MPI-ESM-LR model at all station points and the TSMS observations.

3.2.2.2 Precipitation

The pointwise annual bias distribution over the time period 1971-2005 is shown for 0.11° simulation (Figure 3.26). The mean bias is around 178 mm when averaged over the whole stations dependent on the observational dataset. The overall bias is mainly generated along a band from northeast to western part of the domain. The maximum wet bias is observed in 17072 Duzce station with 758.3 mm. At this point, the model elevation is 358 meters higher than station's elevation. On the contrary, maximum negative bias is estimated in 17186 Manisa station, which is located in western Turkey, with a value of -343 mm. Beside these, the standard deviation of all points is evaluated as approximately 216 mm.

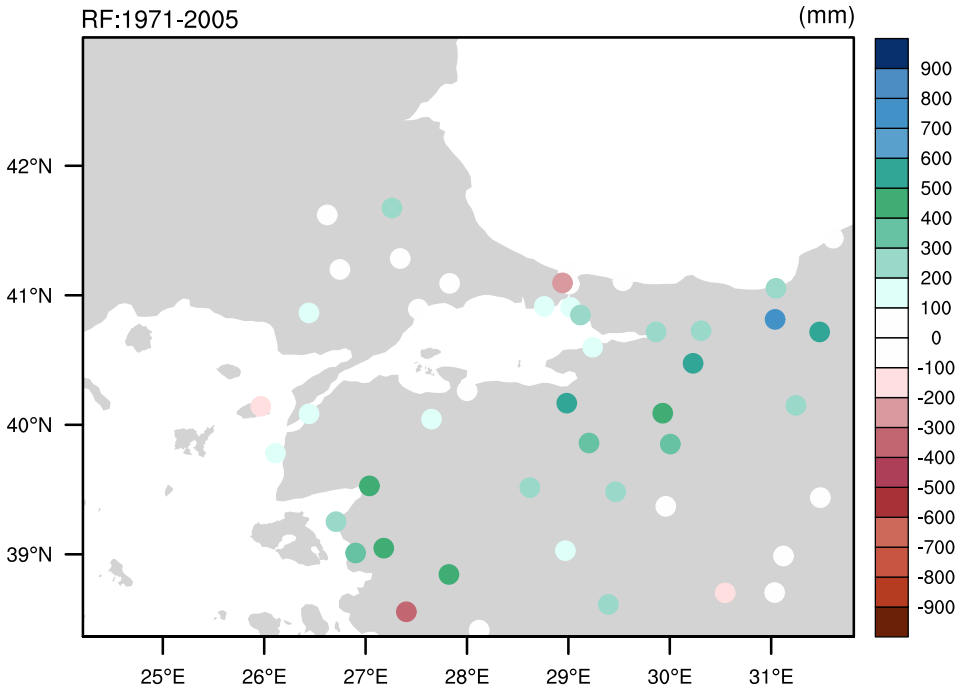

Figure 3.26 : Annual precipitation bias of 0.11° CCLM_MPI-ESM-LR simulations with respect to TSMS observations between 1971-2005 period.

The model shows a much stronger overestimation of precipitation at 0.11° resolution across all seasons, excluding summer (Figure 3.27). The variation range with respect to the mean is wide in winter biases whereas the lowest standard deviation of biases is observed in summer with 39 mm. Additionaly, spring and autumn seasons have 65 and 59 mm standard deviation values, respectively. The mean seasonal bias averaged over each station is shown in (Figure 3.28). The averages of seasonal precipitation differences over all statios are computed as 57.9 mm in winter, 79.5 mm in spring, 24 mm in summer and 15.2 mm in autumn. The spatial patterns exhibit pronounced wet bias along a belt from the norhteastern part to southwestern part of the domain. The bias along this belt surpasses 120 mm in winter season. As like in reanalysis driven CCLM, towards to central Turkey precipitation is simulated quite well with a mean bias between 0 and 80 mm. In summer, differences between the model and TSMS values are lower or even null compared to other seasons. Some exceptions occur in stations located in northeastern part of the domain such as 17072 Duzce, 17116 Bursa and 17662 Geyve stations (Figure 3.28). The overcatchment of precepitation exceeds 90 mm over these stations and also elevation differences between the model and stations are over 325 meters.

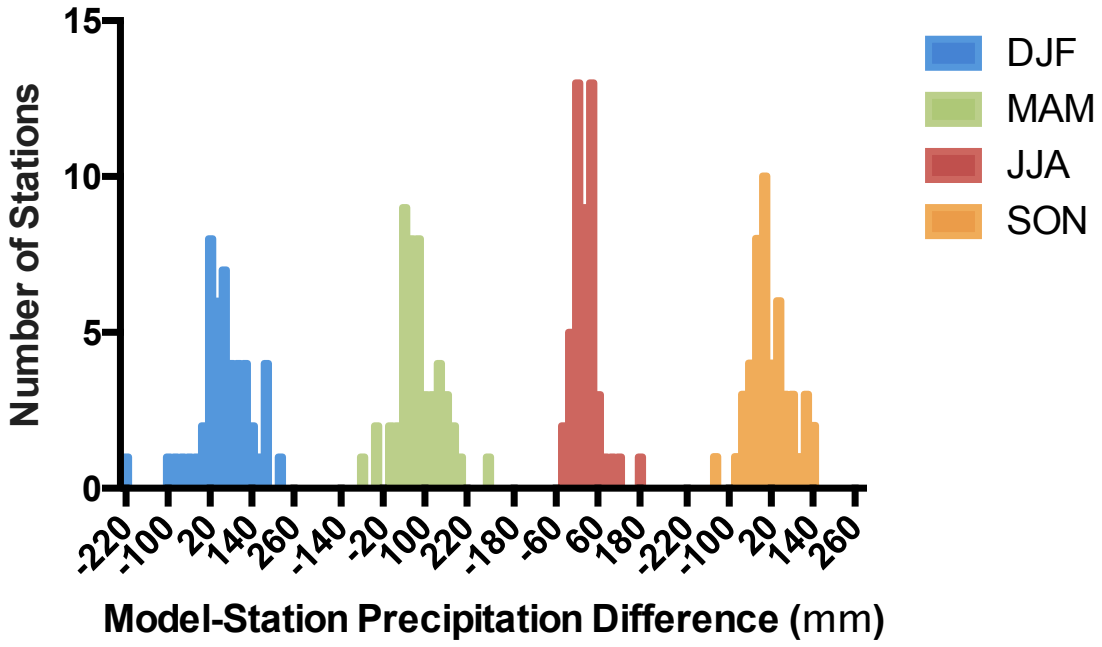

Figure 3.27 : The distribution of the seasonal total precipitation differences between the CCLM_MPI-ESM-LR model at all station points and the TSMS observations.

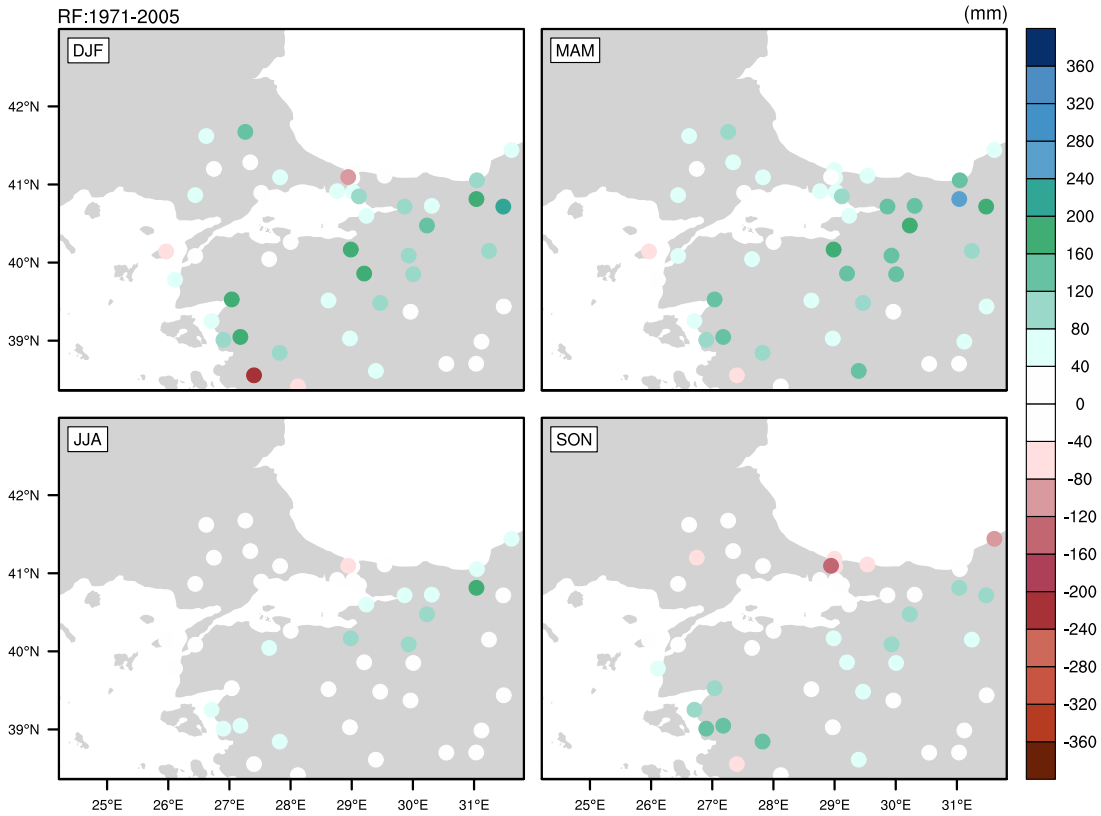

Figure 3.28 : Seasonal precipitation bias of 0.11° CCLM_MPI-ESM-LR simulations with respect to TSMS observations between 1971-2005 period.

The spatial distribution of 35-year contribution of seasonal total precipitation to annual total precipitation is shown in Figure 3.29. Winter season has the largest contribution to annual totals for both station observations and CCLM_MPI-ESM-LR simulations. When the model is compared with TSMS stations (Figure 3.29-a), it is seen that the model (Figure 3.29-b) undercatches the winter contribution specifically over Aegean Region. The contribution of winter, which is calculated from TSMS observations, lies between 25% and 50% all over the study area whereas the contribution of simulated winter ranges from 25% to 45%. Moreover, the contribution of other seasons over Aegean Region generally overpredicted by CCLM_MPI-ESM-LR model. When the whole domain is considered for both observation and simualtation, it is seen that the contribution of the other seasons usually is not larger than 35%. However, the contribution values of spring that is simulated by the model exceed 40% over central Turkey. On one hand, the simulated spring season (Figure 3.29-b) contribute to the annual amounts at least 5% more than observed spring season (Figure 3.29-a) almost all over the domain. On the other hand, the simulated autumn season contribute to annaul amounts aproximately 5% less than observed autumn season.

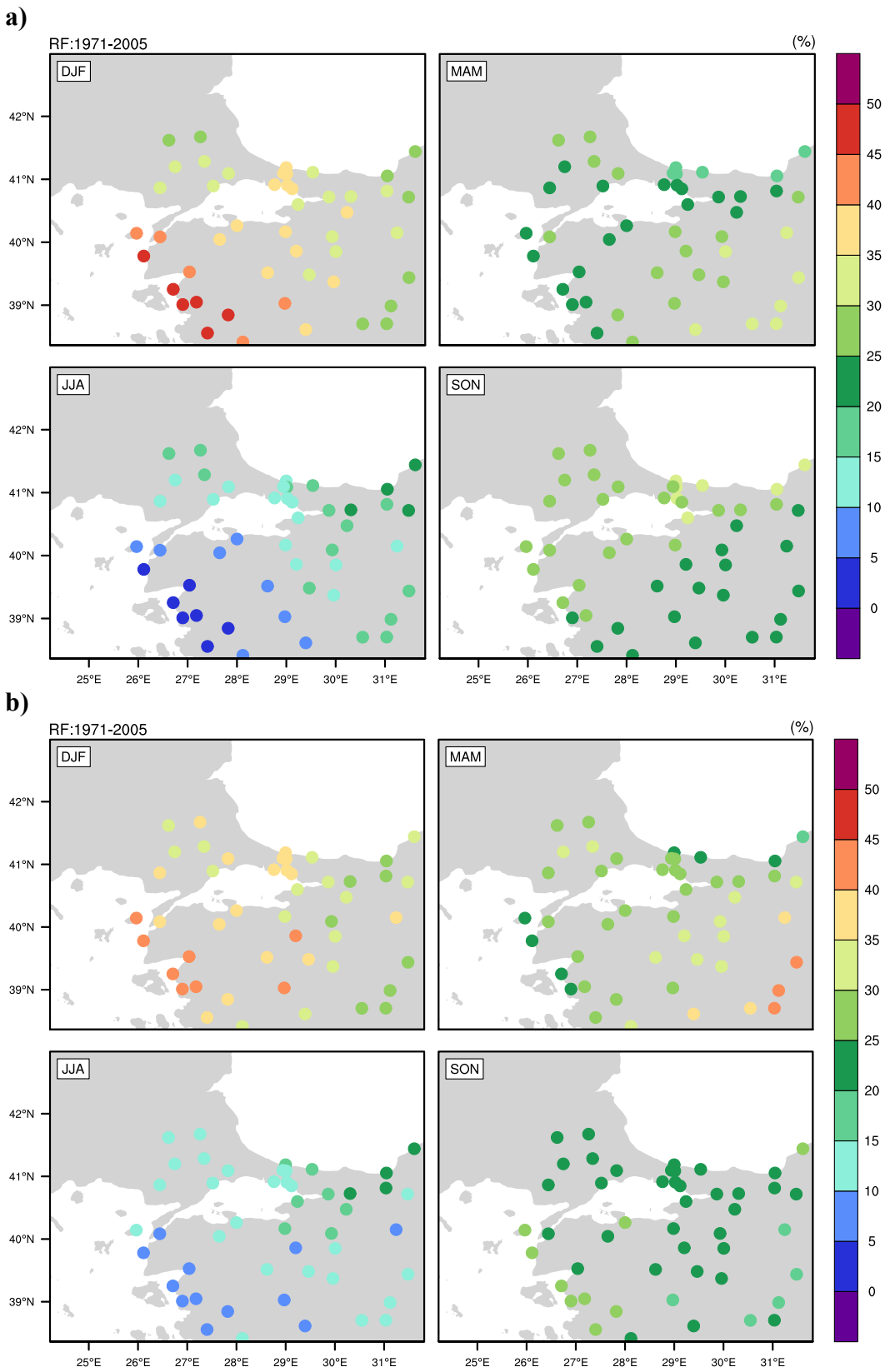

Figure 3.29 : Contribution of seasonal to annual total precipitation calculated from **a)** TSMS stations, **b)** 0.11° CCLM_MPI-ESM-LR simulations for 1971-2005 reference period.

3.3 Climate Projections for 21st Century

3.3.1 0.44° simulations

The changes in precipitation and mean temperature according to RCP 8.5 emission scenario are presented in order to comprehand their trends till the end of 21st century. The variables were obtained from 0.44° resolution model simulation and their variations with respect to reference period were analyzed by dividing the whole time period into three parts; 2011-2040, 2041-2070 and 2071-2100. First column of the figures displays 1971-2005 climatology and the others show changes in variables for corresponding time interval relative to the reference period.

3.3.1.1 Temperature

As can be inferred from Figure 3.30, the average temperature values have increased conspicuously over the study area for both 2041-2070 period and 2071-2100 period. The winter temperature changes over the entire domain are less than the summer temperature changes during all periods. Especially in the spring months, the warming rates between west and east of Turkey are different. The surface albedo increases due to the fact that the snow cover starts to decrease before the spring. This leads to a further increase in temperatures over Eastern Anatolia. Black Sea and its vicinity are exposed to cooling in the winter of 2011-2040 period. The warming is only seen over the southern part of Turkey and Europe and usually varies between 0℃ and 0.5℃. After 2011-2040 period, there is temperature increase of 3℃ over the Mediterranean coastal strip, South Aegean and Southeastern Anatolia regions. Furthermore, climate projections between 2071 and 2100 show significant warming (>6°C) particularly over eastern and southeastern part of Turkey in summer. Rising mean temperatures over these areas, where the average summer temperatures are already high, implies that the frequency and severity of extreme weather events such as heat waves that occurs mostly in summer months would increase. Moreover, long periods of summer drought would turn the areas that are already sensitive to fire into permanent hazardous areas (IPCC, 1995). In addition, another IPCC report propounds that due to the increase in emergence of high fire danger days and in fire season length, future wildfire risk increases (2014).

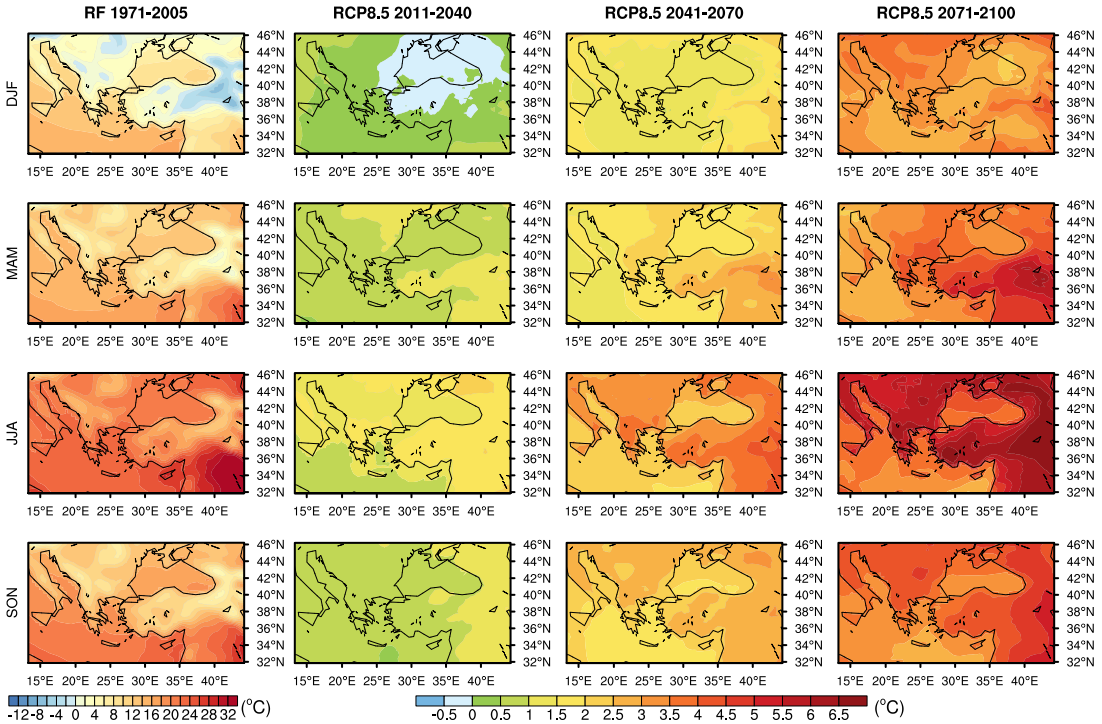

Figure 3.30 : The seasonal average temperatures for RF (1971-2005) and the seasonal model anomaly (2011-2100 period) of RCP8.5 on 30-year basis.

3.3.1.2 Precipitation

Seasonal changes in total precipitation for thirty-years periods with respect to reference climatology under the RCP8.5 scenario are displayed in Figure 3.31. In general, it is understood that the total precipitation tends to decrease for all thirty-years periods. It is also observed that the intensity of the decrement is strengthened towards the end of the century. For instance, as can be seen in the winter season, it is estimated that precipitation will decrease around 40 mm on the Mediterranean coast in 2011-2040 period while precipitation expectations in the last period indicate dramatic decrease (over -150 mm) along Mediterranean region, including southern and eastern part of Turkey. The opposite is expected on the coast of the Black Sea facing Georgia. In some parts of this region, total precipitation is predicted to be more than 150 mm compared to the 1971-2005 reference period. These wet conditions are more apparent towards to the end of 21st century and dominates also the northeastern part of Turkey. Unlike other seasons, positive changes in precipitation are prevalent over Mediterranean region in fall during the period of 2011-2040.

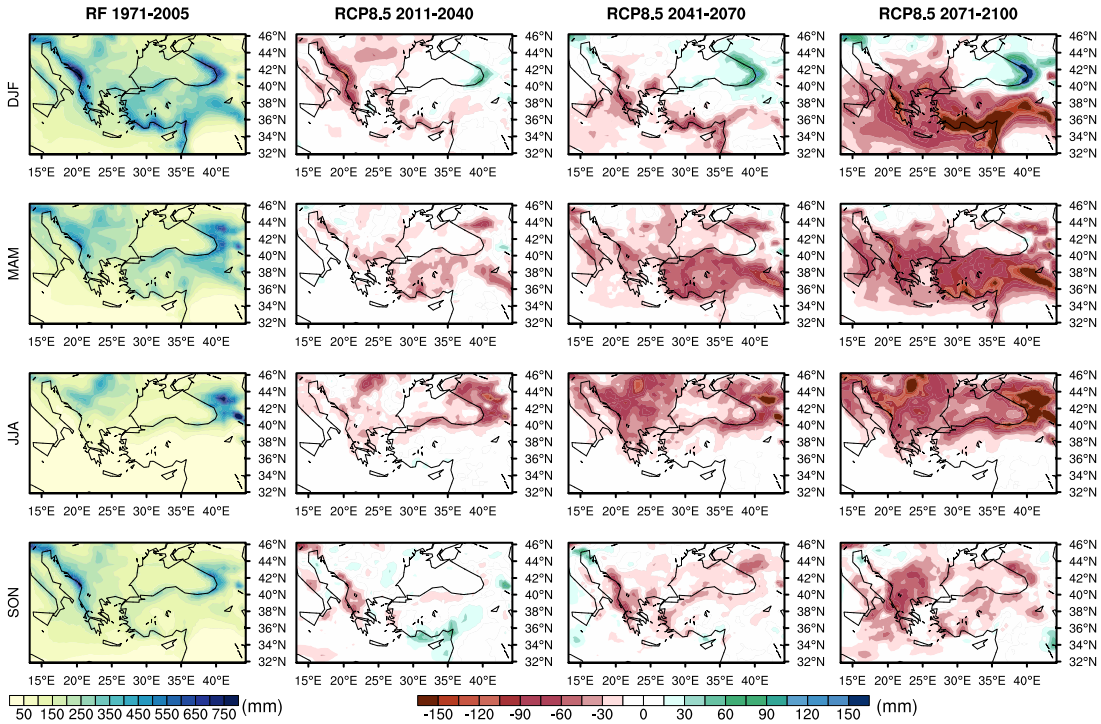

Figure 3.31 : The seasonal total precipitation for RF (1971-2005) and the seasonal model anomaly (2011-2100 period) of RCP8.5 on 30-year basis.

3.3.2 0.11° simulations

For the period between 2011 and 2100, changes in the total precipitation and mean temperature and their general trends are presented based on thirty-years seasonal averages calculating from 0.11 degree model simulations according to the RCP 8.5 scenario. First column of the figures shows 1971-2005 climatology whereas the others present changes in variables for corresponding time interval with respect to the reference period.

3.3.2.1 Temperature

As can be seen on Figure 3.32, the projected changes of 2-m air temperature are positive for the entire domain, which covers northwestern Turkey, in both all seasons and all periods, excluding the winter season of first 30-year period. After the mid-century, warming is expected to accelerate expecially in summer season. Anomolous warming in summer is expected over central region of Turkey towards to the end of century. During the last thirty-years period this warming exceeds over 6°C while the lowest increase (approximately 3°C) is expected to occur in the winter season. Furthermore, the highest temperature increase is seen generally in spring and

summer seasons for all three periods. In most of the periods, Istanbul is warmer than in the Asian and European part of the domain.

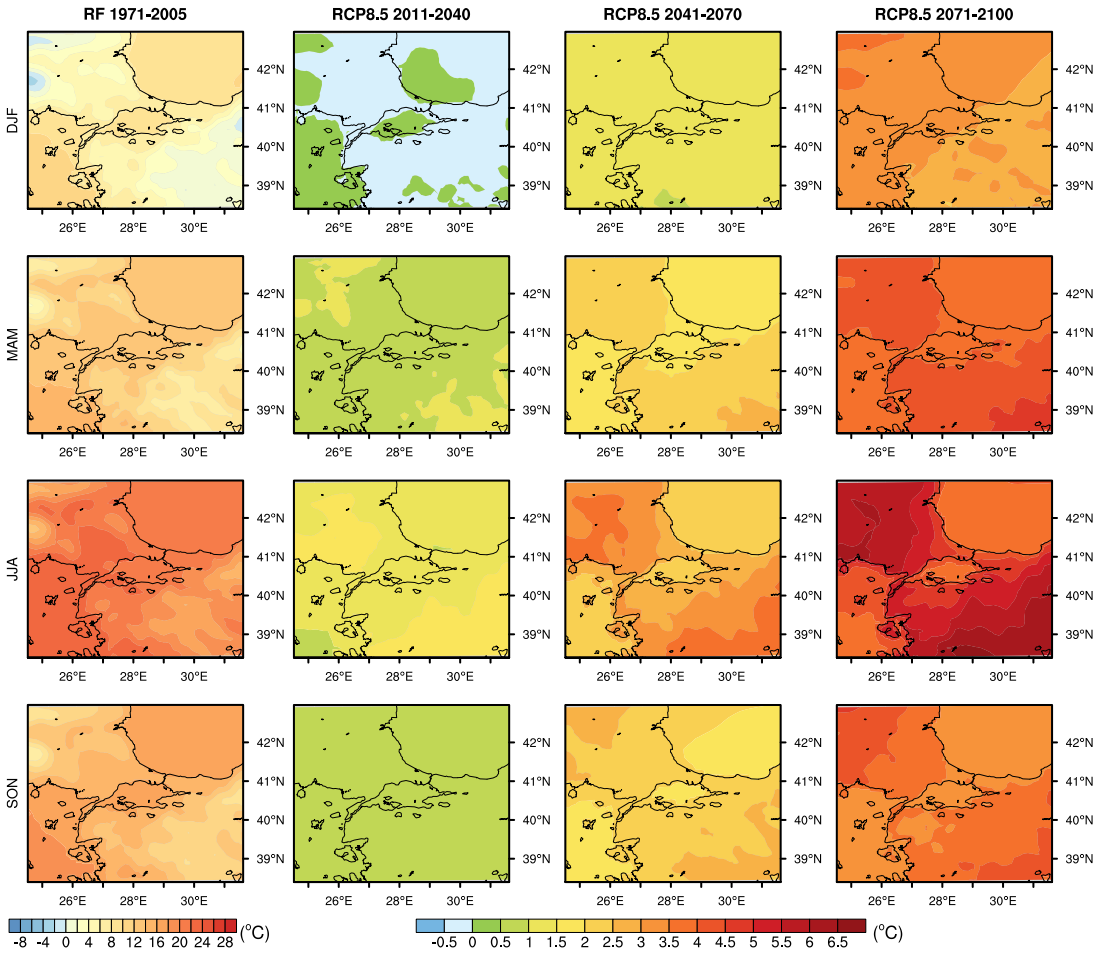

Figure 3.32 : The seasonal average temperatures for RF (1971-2005) and the seasonal model anomaly (2011-2100 period) of RCP8.5 on 30-year basis.

3.3.2.2 Precipitation

The variation of the precipitation regime over the period 2011-2100 in accordance with the RCP 8.5 scenario for 0.11° resolution is displayed with Figure 3.33. The most pronounced changes in the precipitation patterns over the model domain is seen in spring and summer seasons as it is seen in temperature. In each period, the CCLM model simulates averagely less than 60 mm of precipitation around the Rhodope Mountains in Bulgaria compared to the reference period. Besides, the drought over mountainous regions reaches extreme levels in the last period. For instance, it is expected that the total amount of precipitation in the summer will decrease by 150 mm over the Köroğlu Mountains, where the altitude is up to 3000 meters. This anomolous decrease in precipitation shows similar pattern over Mount Ida, Uludağ and Rhodope Mountains. Contrary to this situation, the CCLM model generates

positive anomaly values over Bolu mountains in winter seasons of 2041-2070 and 2071-2100 periods.

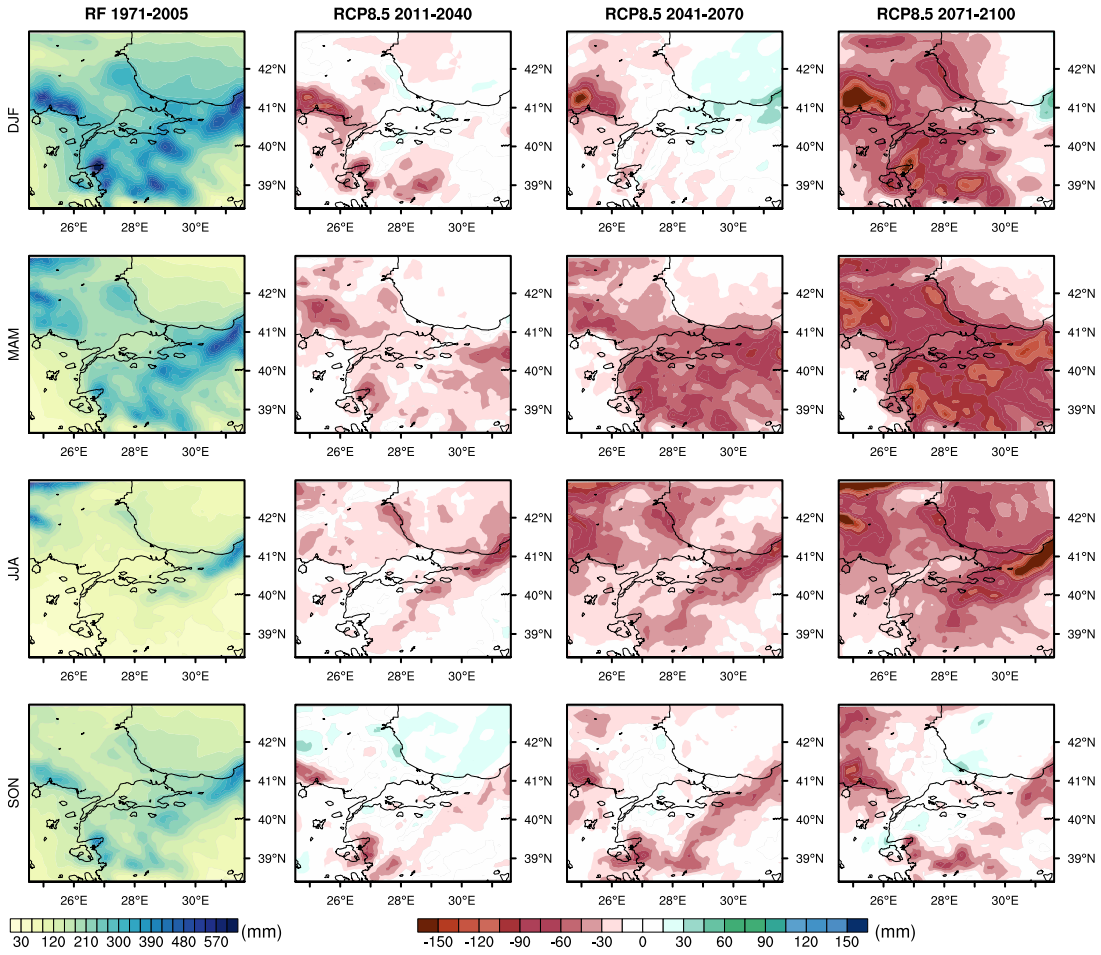

Figure 3.33 : The seasonal total precipitation for RF (1971-2005) and the seasonal model anomaly (2011-2100 period) of RCP8.5 on 30-year basis.

4. CONCLUSIONS AND RECOMMENDATIONS

The simulations represent the longest regional climate analyses for Turkey based on non-hydrostatic CCLM model at such a high spatial and temporal detail. The aims of this study are to test the performance of the model in capturing temperature and precipitation climatology and to explore the future changes in surface climate variables through 21st century by employing RCP8.5 scenario. The evaluation simulations cover the reference time period of 35 years and approximately 90 years for future projections.

Firstly, the CCLM simulations having 0.44° resolution are validated with respect to CRU data for 1971-2005 reference period. In general, the performance of both CCLM_NCEP1 and CCLM_MPI-EMS-LR is good at capturing 2-m temperature pattern. Annual averages become more consistent (around ± 1℃) over Turkey after coupling with MPI-EMS-LR. The seasonal and interannual variability of the coupled system is lower than the NCEP1 driven CCLM simulations in almost everywhere of the domain. The standard deviation biases over Turkey and Europe are calculated approximately 0.6℃ and -0.7℃ respectively for CCLM_NCEP1 and CCLM_MPI-EMS-LR. The winter and autumn temperature biases ranges between -2℃ and 1℃ over Turkey but the bias values approach to zero (± 1℃), when the model is coupled with MPI-ESM-LR. In winter and spring, high-elevation warming, which the model produce at least 2℃ higher temperatures than CRU, appears in both performance simulations. This would be related with the number of snow days and the snow-albedo feedback. In contrast, the model produces lower temperatures (<-2℃) generally over northeastern part of Turkey with respect to CRU data.

High consistency (± 100 mm) with precipitation observations is seen over northern Turkey in reanalysis driven model results, likewise, over southern Turkey in MPI-ESM-LR coupled model results. Both 0.44° simulations have wet biases that exceed 800 mm annual total precipitation of CRU data over Caucasus Mountain. Bozkurt (2012) claims that separation of the northerly flow into two parts by high Anatolian Peninsula brings about abundant precipitation along the mountains of northeastern

Turkey and Caucasus. CCLM_NCEP1 simulates noticeable negative bias over coastal regions of Mediterranean Sea compared to CCLM_MPI-ESM-LR for both annual and seasonal basis. The coupling with MPI-ESM-LR has changed the standard deviation biases from negative to positive over the western coast of the land areas in which COSMO_NCEP1 produced significantly less variability compared to CRU observations. The both model simulations are generally more consistent (± 50 mm) over Turkey in summer season. CCLM_NCEP1 produces usually close values to observations in winter and spring while CCLM_MPI-ESM-LR predicts consistent values in summer and autumn for whole domain.

Secondly, CCLM simulations with 0.11° resolution are tested according to meteorological observations obtained from 48 TSMS stations. When the model results are compared with TSMS stations on annual and seasonal basis, it is concluded that temperature changes commonly show a strong elevation dependency in many stations. However, the details mostly depend on the season. After applying elevation correction, the annual biases that are averaged over all 48 stations are reduced from -1.3℃ to -0.5℃ for CCLM_NCEP1 and from -0.49℃ to 0.3℃ for CCLM_MPI-ESM-LR. Nevertheless, temperature simulations of the coupled system are more consistent on annual and seasonal basis than reanalysis driven simulations except for summer season. Moreover, it decreases negative temperatures biases that is produced by CCLM_NCEP1 mostly in winter and autumn seasons at least 1℃. Variation range becomes narrower and extreme values disappear after the elevation correction.

CCLM_NCEP1 produces generally lower precipitation while CCLM_MPI-ESM-LR simulates higher precipitation than TSMS stations. The annual bias averaged over all stations is calculated as -180.6 mm and 177.8 mm, respectively from reanalysis driven and ESM coupled model results, respectively. The best performance is occurred in the summer season (± 25 mm) for both simulations. The coupled model system is highly skilled in simulating the precipitation in summer (24 mm) and autumn (15.2 mm) seasons whereas the reanalysis driven model system is highly skilled in simulating the precipitation in spring (0.7 mm) and summer (-16 mm). In all seasons, the both CCLM_MPI-ESM-LR and CCLM_NCEP1 are more sensitive throughout the inland parts of Turkey.

Finally, the analyses of the projected changes in accordance with RCP8.5 scenario suggest that the CCLM model forced with MPI-ESM-LR predicts increasing temperatures towards to the end of 21st century although the cooling that ranges between -0.5℃ and 0℃ is expected in the winter of 2011-2040 period. According to both 0.44° and 0.11° resolutions, the summer season is affected from climate change more dramatically. During the last 30-year period this warming exceeds 6℃ in the summer while the lowest increase (approximately 3℃) is expected to occur in the winter season. This distinctive warming rates between winter and summer were also presented in Onol and Semazzi (2009), Unal et al. (2006-2010) and Onol et al. (2014). For the last 30-year period of all seasons excluding winter, the central Turkey might be under the influence of dramatic rising temperatures (>3.5℃) with respect to 0.11° simulations while eastern and southern part of Turkey might be also dominated by significant warming (>3.5℃) according to 0.44° simulations.

For both resolution results, the drought in the second half of the century is predicted to accelerate more steeply. The decreasing precipitation exceeds 150 mm especially in the summer season. The previous studies such as Onol et al. (2014) and Bucchignani et al. (2016) agree that the significant precipitation reduction is expected to occur in summer season. But in the winter, wet conditions are apparent on the coast of the Black Sea facing Georgia and over northern Italy. It is also consistent with RCP8.5 projections of Bucchignani et al. (2016). Besides, Mediterranean region is dominated by dramatic decrease in precipitation while Black Sea region faces with wet conditions in the winter, which was also reported by Onol and Semazzi (2009), Unal et al. (2006-2010) and Onol et al. (2014). Moreover, the model run with 0.11° resolution produces drier conditions over mountainous regions in the last 30-year period compared to previous periods.

REFERENCES

Bartholome, E., Belward, A. S., Achard, F., Bartalev, S., Carmonamoreno, C., Eva, H., ... Stibig, H-J. (2002). *GLC 2000 Global Land Cover mapping for the year 2000 Project status November 2002.* Institute for Environment and Sustainablity. European Communities.

Beguería, S., Vicente-Serrano, S. M., Tomás-Burguera, M., & Maneta, M. (2015). Bias in the variance of gridded data sets leads to misleadingconclusions about changes in climate variability. *Int. J. Climatol., 36*, 3413-3422.

Bozkurt, D., & Sen, O. (2011). Precipitation in the Anatolian Peninsula: sensitivity to increased SSTs in the surrounding seas. *Climate Dynamics, 36* (3), 711-726.

Bozkurt, D., Turuncoglu, U., Sen, O. L., Onol, B., & Dalfez, H. N. (2012). Downscaled simulations of the ECHAM5, CCSM3 and HadCM3 global models for the eastern Mediterranean–Black Sea region: evaluation of the reference period. *Climate Dynamics, 39* (1), 207-225.

Bucchignani, E., Cattaneo, L., Panitz, H. J., & Mercogliano, P. (2016). Sensitivity anaysis with the regional climate model COSMO-CLM over CORDEX-MENA domain. *Meteorol. Atmos. Phys.*, 73-95.

Bucchignani, E., Montesarchio, M., Zollo, A. L., & Mercogliano, P. (2016). High-resolution climate simulations with COSMO-CLM over Italy: performance evalution and climate projections for 21st century. *International Journal of Climatology, 36*, 735-756.

COSMO. (2011, August). *Lateral Boundaries and Driving Models*. Retrieved October 2016, from Consortium for Small-scale Modeling: http://www.cosmo-model.org/content/model/int2lm/default.htm

Davies, H. C. (1976). A lateral boundary formulation for multi-level prediction models. *Quart. J. R. Met. Soc., 102*, 405–418.

Dee, Dick, Fasullo, John, Shea, Dennis, ... National Center for Atmospheric Research Staff. (2016, Jan 21). *The Climate Data Guide: Atmospheric Reanalysis: Overview & Comparison Tables*. Retrieved 2016, from https://climatedataguide.ucar.edu/climate-data/atmospheric-reanalysis-overview-comparison-tables

Doms, G., & Baldauf, M. (2015). Part I: Dynamics and Numerics. In *A Description of the Nonhydrostatic Regional COSMO-Model* (pp. 1-158). Offenbach, Germany: Deutscher Wetterdienst.

FAO-Unesco. (1974). *Soil map of the world.* Paris: United Nations Educational, Scientific and Cultural Organization.

GACP. (2016, January). *Global Aerosol Climatology Project*. Retrieved September 2016, from National Aeronautics and Space Administration Goddard Institute for Space Studies: http://gacp.giss.nasa.gov/

Gal-Chen, T., & Sommerville, C. (1975). On the use of a coordinate transform for the sulution of the Navier-Stokes equations. *J. Comput. Phys., 17*, 209-228.

Geyer, B. (2014). High-resolution atmospheric reconstruction for Europe 1948–2012: coastDat2. *Earth Syst. Sci. Data, 6*, 147–164.

Giorgetta, M. A., Jungclaus, J., Reick, C. H., Legutke, S., Bader, J., Böttinger, M., ... Stevens, B. (2013). Climate and carbon cycle changes from 1850 to 2100 in MPI-ESM simulations for the Coupled Model Intercomparison Project phase 5. *Journal of Advances in Modelling Earth Systems, 5* (3), 572-597.

Giorgi , F., Hurrell, J. W., & Marinucci, M. R. (1997). Elevation dependency of the surface climate change signal: a model study. *Clim. Change, 10*, 288-296.

Giorgi, F. (2006). Climate change hot-spots. *Geophys. Res. Lett., 33*, L08707.

Gobiet, A., Kotlarski, S., Beniston, M., Heinrich, G., Rajczak, J., & Stoffel, M. (2014). 21st Century Climate Change in the European Alps - A Review. *Science of the Total Environment, 493*, 1138-1151.

Harris, I., Jones, P. D., Osborn, T. J., & Lister, D. H. (2014). Updated high-resolution grids of monthly climatic observations – the CRU TS3.10 Dataset . *International Journal of Climatology, 34* (3), 623-642.

Hatzianastassiou, N., Papadimas, C. D., Lolis, C. J., Bartzokas, A., Levizzani, V., Pnevmatikos, J. D., ... Katsoulis, B. D. (2016). Spatial and temporal variability of precipitation over the Mediterranean Basin based on 32-year satellite Global Precipitation Climatology Project data, part I: evaluation and climatological patterns. *Int. J. Climatol., 36*, 4741–4754.

IPCC. (1995). *Climate Change 1995: The IPCC Second Assessment Report.* Contribution of Working Group II of the Intergovernmental Panel on Climate Change, forming part of the IPCC Second Assessment Report. Cambridge University Press.

IPCC. (2014). *Climate Change 2014: Impacts, Adaptation, and Vulnerability. Part A: Global and Sectoral Aspects. Contribution of Working Group II to the Fifth Assessment Report of the Intergovernmental Panel on Climate Change.* Cambridge, United Kingdom and New York, NY, USA: Cambridge University Press.

Jacob, D., Petersen, J., Eggert, B., Alias, A., Christensen, O. B., Bouwer, L. M., ... Yiou, P. (2014). EURO-CORDEX: new high-resolution climate change projections for European impact research. *Reg. Environ. Change, 14*, 563–578.

Jaeger, E. B., Anders, I., Lüthi, D., Rockel, B., Schär, C., & Seneviratne, S. (2008). Analysis of ERA40-driven CLM simulations for Europe. *Meteorologische Zeitschrift, 17*, 349-367.

Joint Research Centre. (2003). *Global Land Cover 2000 database*. Retrieved February 2016, from European Commision, Joint Research Centre: http://forobs.jrc.ec.europa.eu/products/glc2000/glc2000.php

Karaca, M., Unal, Y. S., Kındap, T., & Dalfes, N. (2003). *Küresel iklim değişimi ve GAP bölgelerine yansımaları.* DPT Projesi.

Kotlarski, S., Bosshard, T., Lüthi, D., Pall, P., & Schar, C. (2012). Elevation gradients of European climate change in the regional climate model COSMO-CLM. *Climatic Change, 112*, 189-215.

Liu, X. -D., Osher, S., & Chan, T. (1994). Weighted essentially non-oscillatory schemes. *J. Comput. Phys., 115*, 200–212.

Meissner, C., Schadler, G., Panitz, H. -J., Feldmann, H., & Kottmeier, C. (2009). High-resolution sensitivity studies with the regional climate model COSMO-CLM. *Met. Z., 18*, 543-557.

MGM. (2015). *Yeni senaryolar ile Türkiye İklim Projeksiyonları ve iklim değişikliği, TR2015-CC.* Ankara: Araştırma Dairesi Başkanlığı, Meteoroloji Genel Müdürlüğü.

Moss, R. H., Edmonds, J. A., Hibbard, K. A., Manning, M. R., Rose, S. K., van Vuuren, D. P., ….. Wilbanks, T. J. (2010). The next generation of scenarios for climate change research and assessment. *Nature, 463*, 747–756.

Murphy, J. (1999). An evaluation of statistical and dynamical techniques for downscaling local climate. *J Climate, 12*, 2256– 2284.

Onol, B. (2012). Effects of coastal topography on climate: high-resolution simulation with a regional climate model. *Clim. Res., 52*, 159-174.

Onol, B., & Semazzi, F. (2009). Regionalization of climate change simulations over the eastern Mediterranean. *Journal of Climate, 22*, 1944-57.

Onol, B., & Unal, Y. (2014). Assessment of climate change simulations over climate zones of Turkey. *Regional Environmental Change, 14* , 1921-1935.

Onol, B., Bozkurt, D., Turuncoglu, U. U., Sen, O. L., & Dalfes, H. N. (2014). Evaluation of the twenty-first century RCM simulations driven by multiple GCMs over the Eastern Mediterranean–Black Sea region. *Clim. Dyn., 42*, 1949–1965.

Ritter, B., & Geleyn, J. F. (1992). A comprehensive radiation scheme for numerical weather prediction models with potential applications in climate simulations. *Mon. Wea. Rev., 120*, 303-325.

Roesch, A., Jaeger, E. B., Lüthi, D., & Seneviratne, S. I. (2008). Analysis of CCLM model biases in relation to intra-ensemble model variability. *Meteorologische Zeitschrift, 17*, 369-382.

Schär, C., Leuenberger, D., Fuhrer, O., Lüthi, D., & Girard, C. (2002). A new terrain-following vertical coordinate formulation for atmospheric prediction models. *Mon. Wea. Rev., 130*, 2459-2480.

Schättler, U., Doms, G., & Schraff, C. (2016). Part VII : User's Guide. In *A Description of the Nonhydrostatic Regional COSMO-Model* (pp. 1-221). Offenbach, Germany: Deutscher Wetterdienst.

Skamarock, W. C., & Klemp, J. B. (1992). The stability of time-split numerical methods for the hydrostatic and the nonhydrostatic elastic equations. *Mon. Wea. Rev., 120*, 2109–2127.

Sommeria, G., & Deardorff, J. W. (1977). Subgrid-scale condensation in models of non-precipitating clouds. *J. Atmos. Sci., 34*, 344-355.

Thomas, S., Girard, C., Doms, G., & Schättler, U. (2000). Semi-implicit scheme for the DWD Lokal-Modell. *Meteor. Atmos. Phys., 75*, 105–125.

Tiedtke, M. (1989). A comprehensive mass flux scheme for cumulus parameterization in large-scale models. *Mon. Weather Rev. , 117*, 1779-1799.

Unal, Y. S., Önol, B., Karaca, M., & Dalfes, N. (2001). *Climate of the Southeastern Anatolia Project (GAP) Basin for 21st Century by Meso Scale Model.* ITU Research Foundation Project.

Unal, Y. S., Önol, B., Menteş, S., Borhan, Y., Kahraman, A., & Ural, D. (2006-2010). *Assessment of Global Climate Change Impact on Turkey by Regional Climate Model.* TUJJB-TUMEHAP, TUJJB (Union of Turkish National Geodesy and Geophysics).

University of East Anglia Climatic Research Unit. (2015, Noverber 9). *CRU TS3.23: Climatic Research Unit (CRU) Time-Series (TS) Version 3.23 of High Resolution Gridded Data of Month-by-month Variation in Climate (Jan. 1901- Dec. 2014)*. Retrieved August 2016, from Centre for Environmental Data Analysis: http://dx.doi.org/10.5285/4c7fdfa6-f176-4c58-acee-683d5e9d2ed5

Von Storch, H., Langenberg, H., & Feser, F. (2000). A spectral nudging technique for dynamical downscaling purposes. *Mon. Weather Rev., 128*, 3664–3673.

Wicker, L., & Skamarock, W. (2002). Time-splitting methods for elastic models using forward time schemes. *Mon. Wea. Rev., 130*, 2088–2097.

CURRICULUM VITAE

Name Surname **:** Cemre YÜRÜK

Place and Date of Birth **:** Istanbul, 27.09.1991

E-Mail **:** yurukc@itu.edu.tr

EDUCATION **:**

- **B.Sc.** **:** 2014, Istanbul Technical University, Faculty of Aeronautics and Astronautics, Department of Meteorological Engineering

PROFESSIONAL EXPERIENCE AND REWARDS:

- 2014-date European Union Project, ERANET, LOCLIM3-Local climate change in 3 cities: Cairo, Nairobi, Istanbul, funded by TUBITAK (The Scientific and Technological Research Council of Turkey)
- 2015 Impact of Climate Change on Water Resources Project, *Turkish Ministry of Forestry and Water Affairs*

PUBLICATIONS, PRESENTATIONS AND PATENTS ON THE THESIS:

- **Yürük, C.**, and Unal Y. 2016: Changes in Temperature Extremes in High Resolution Simulations of COSMO-CLM Driven by MPI-ESM-LR Under RCP8.5 Scenario over The Western Part Turkey. MedCLIVAR 2016 Conference, September 26-30, 2016 Athens, Greece.
- **Yürük, C.**, Unal Y., Bilgen S. İ., Topçu S., and Mentes S. 2016: Determining Heat Waves from Observations and COSMO-CLM Simulations in Istanbul. European Geosciences Union General Assembly, April 17-22, 2016 Vienna, Austria.
- Bilgen, S. İ., Unal Y., **Yürük C.**, Goktepe N., Diren D., Topçu S., Mentes S., Incecik S., Güney C., and Doğru, A. Ö. 2016: Investigation of Urban Heat Island Intensity in Istanbul. European Geosciences Union General Assembly, April 17-22, 2016 Vienna, Austria.

- Ünal, Y., Bilgen S. İ., **Yürük C.**, Diren D., İncecik S., Topcu S., Güney C., Dogru A. Ö., Sodoudi S., Langer I., El Zafarany A. M., Abou El Seoud T., and Wesonga J. M. 2015: ERAfrica Project: LOCLIM3 - The local climate changes in 3 cities of Cairo, Nairobi and İstanbul: İstanbul Case. VII. Atmospheric Science Symposium, April 28-30 2015, Istanbul, Turkey, Vol2, p:781-790.
- **Yürük, C.**, Bilgen S. İ., Unal Y., and İncecik S. 2015: Interannual variations of precipitation and temperature observations in Turkey. 5th International Conference on Meteorology and Climatology of the Mediterranean, March 2-4 2015, Istanbul, Turkey.
- Bilgen, S. İ., **Yürük C.**, Goktepe N., Tan E., and Unal Y. 2015: Investigation on Heatwaves over Turkey and Leading Atmopheric Patterns. 5th International Conference on Meteorology and Climatology of the Mediterranean, March 2-4 2015, Istanbul, Turkey.
- **Yürük, C.**, and Unal Y. 2014: Earth System Model Predictions for 2015-2100 over Mediterranean Basin. Climate Change and Climate Dynamics International Conference, October 8-10 2014, Istanbul, Turkey, Proceedings Book of Extended Abstracts, p:9-12. (Presentation Instance)
- Bilgen, S. İ., **Yürük C.**, and Unal Y. 2014: Interannual variability of regional climate model (RegCM) simulations for high and low resolutions over Turkey between 1971 and 2000: Temperature and precipitation. Climate Change and Climate Dynamics International Conference, October 8-10 2014, Istanbul, Turkey, Proceedings Book of Extended Abstracts, p:88-91.